ADCIRC Simulations

Hydrodynamic forcing of the study area included forcing with two types of boundaries. The first applied a time series of water level forcing constructed from the Northeastern Pacific 2002 tidal constituent database at the open ocean boundary.

The second boundary condition was the application of fresh water inflow. Four rivers were used to represent the fresh water inflow into the system. River flow was assumed constant during the simulation period and an average monthly river flow was obtained from the U.S. Geological Survey (USGS) stations at Knik, Matanuska, Susitna and Kenai rivers. River flow was distributed over the nodes along the boundary from which rivers are flowing into the grid. For the run the river inflows were taken to be: Knik, 660 m^3/s, Matanuska, 370 m^3/s, Susitna, 3680 m^3/s, Kenai, 380 m^3/s.

ADCIRC-2DDI simulation was conducted for a time interval of 14 days, August 2-16 2002 (see Figure 17). The run time step was 0.5 sec.

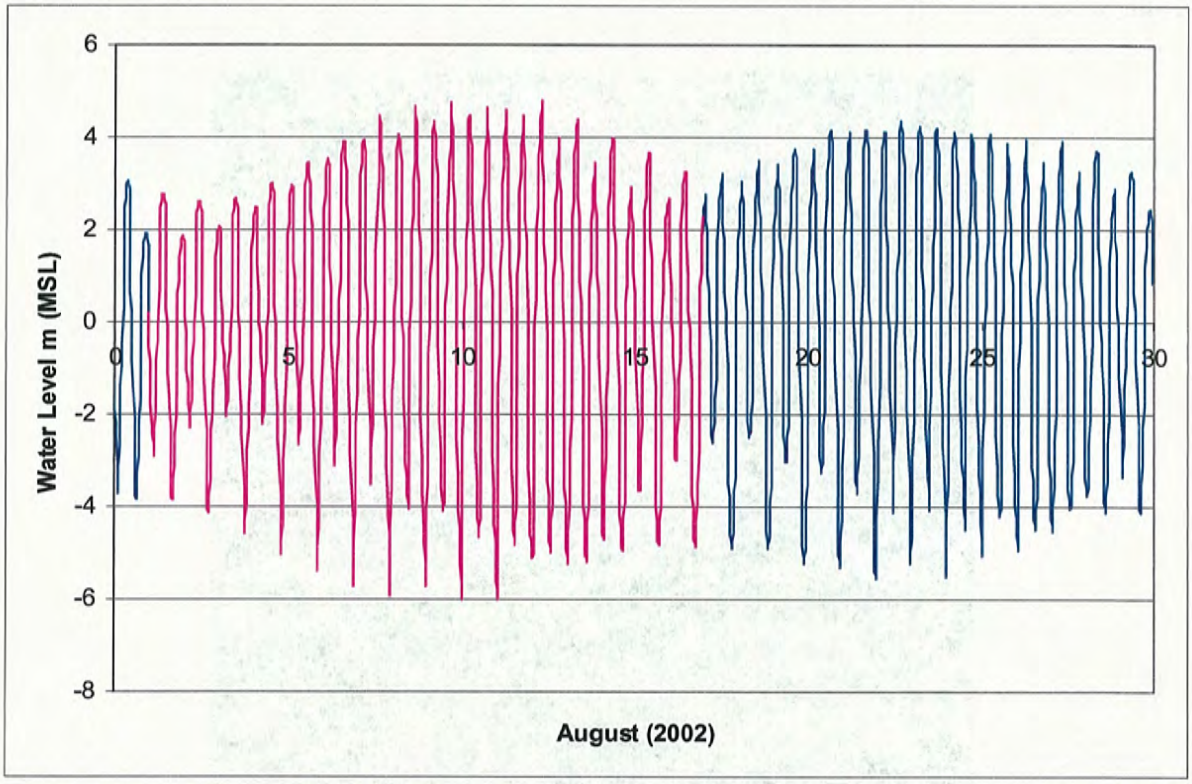

Figure 17 ADCIRC Simulation Period

The friction factor was set to a dimensionless value of 0.0025 throughout the grid. The ADCIRC dimensionless friction factor was increased in the mudflat area to 0.009. This value is obtained by using a Manning coefficient n of 0.04 which is typical for canals and rivers with many stones and weeds (Sabersky *et al.* 1989). The flow is expected to slow down over the flat area. Therefore it was assumed that the high value of Manning coefficient, which was adopted in rivers and canals, would reasonably simulate the friction on the flats, which are characterized by a complex network of small channels.

The dock area has dense pile foundation and a high friction factor should be adopted to slow the flow in the dock area. "There are not enough data and scientific studies to choose the proper friction coefficient to account for large structures. In the absence of proven scientific estimates, we have chosen to use a standard engineering value for Manning parameter corresponding to mildly rough surfaces (n=0.025). The approach gives credible conservative estimate of the tsunami inundation (Vasily *et al.* 2003). Shioyama adopted river channel Manning roughness of 0.035. A Manning coefficient of about 0.055 was adopted at the dock area and a corresponding dimensionless friction factor of 0.02 was set to the nodes within the dock outlined area shown in Figure 18. The same friction factor was also used for the oil terminal nodes.

Figure 18 Nodes with High Friction in the Dock Area

The model was checked by comparing measured and calculated water levels at four NOAA stations shown in Figure 19. Comparison of measured and calculated water level during spring tide of the simulation period at the Anchorage, Nikiski, Seldovia, and Kodiak stations are shown in Figures 20 through 23. The comparison shows very good agreement between measured and calculated water level in the study area.

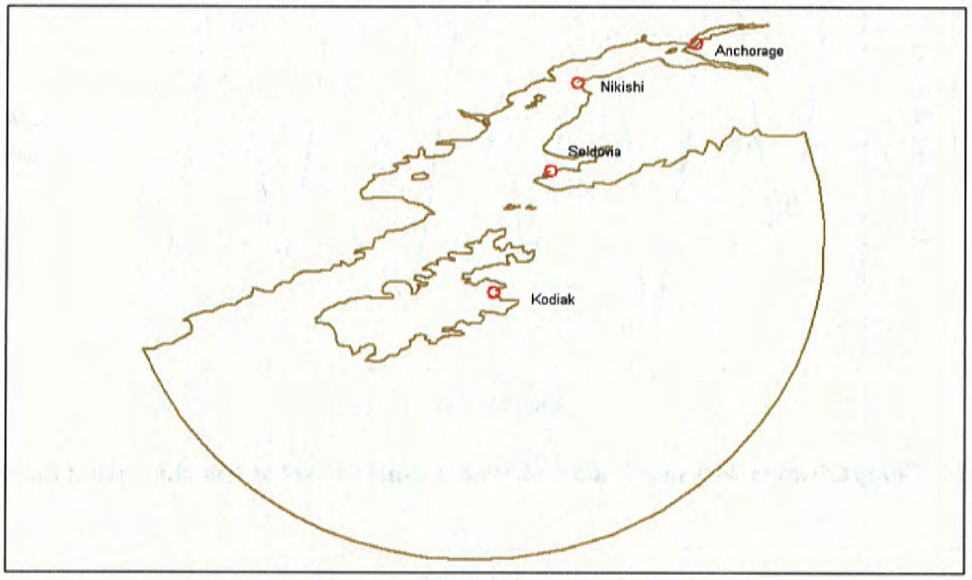

Figure 19 Location of NOAA Stations for Comparison of Measured and Calculated Water Level

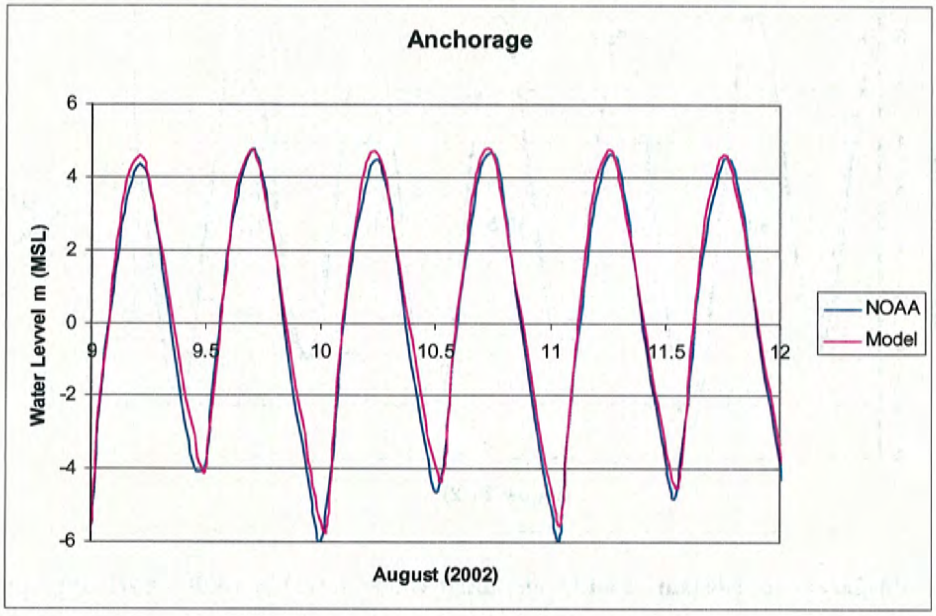

Figure 20 Comparison of Measured and Calculated Water Level at Anchorage During Spring Tide

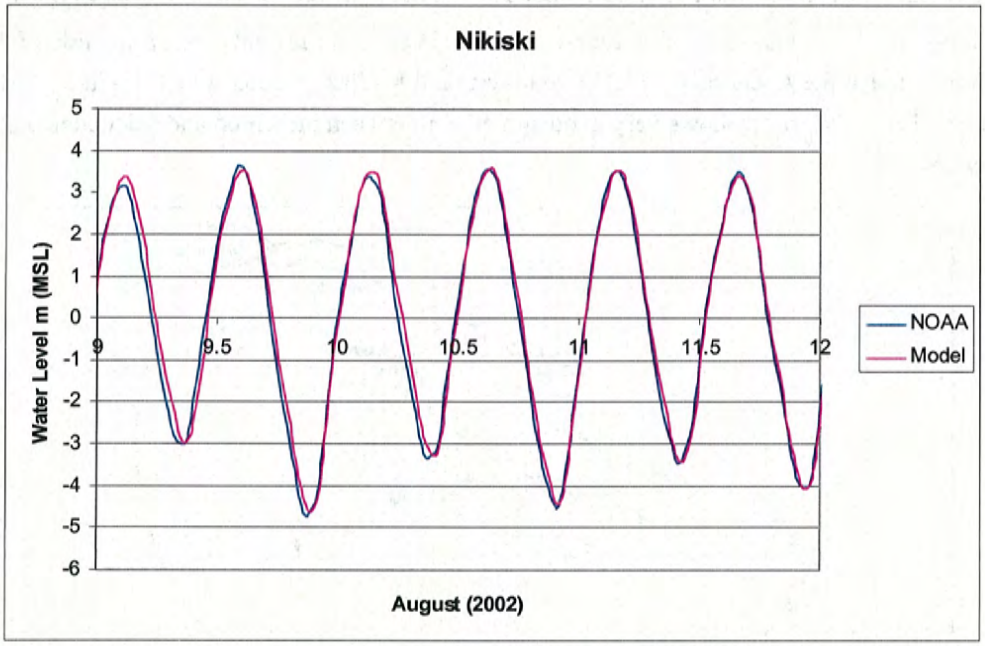

Figure 21 Comparison of Measured and Calculated Water Level at Nikiski During Spring Tide

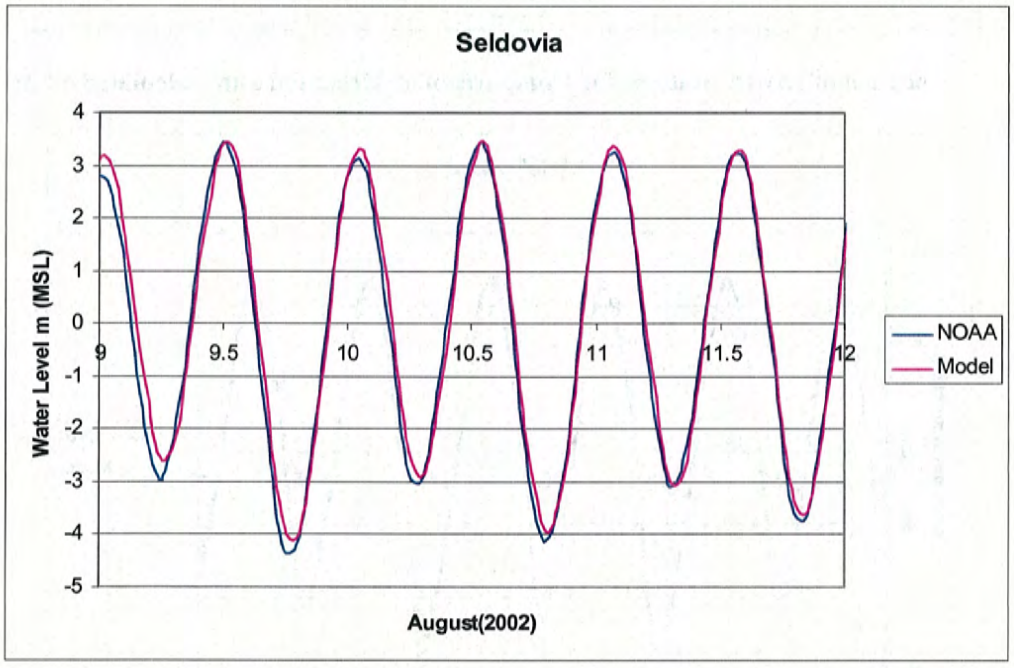

Figure 22 Comparison of Measured and Calculated Water Level at Seldovia During Spring Tide

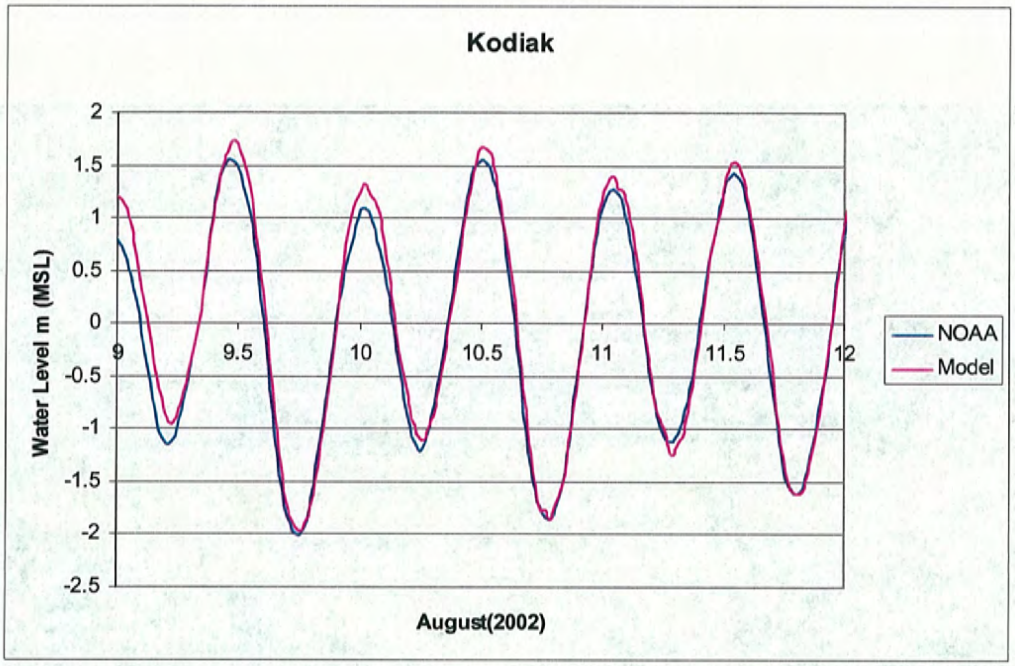

Figure 23 Comparison of Measured and Calculated Water Level at Kodiak During Spring Tide

Port of Anchorage Proposed Expansion

POA expansion activities are anticipated to include several program elements:

- Expanding commercial dock space
- Supporting military rapid deployment from Alaskan bases, including the U.S. Army's Stryker Brigade Combat Team Sealift Operation
- Providing additional barge dock capacity
- Developing a Cruise Ship Terminal
- Improving rail connection to POA for commercial and military use

Figure 24 shows the anticipated six areas of expansion. The present study involves evaluating the tidal circulation changes induced by the presence of the full, proposed Port expansion, which was represented in the model by adding a solid fill to the six areas shown in Figure 24.

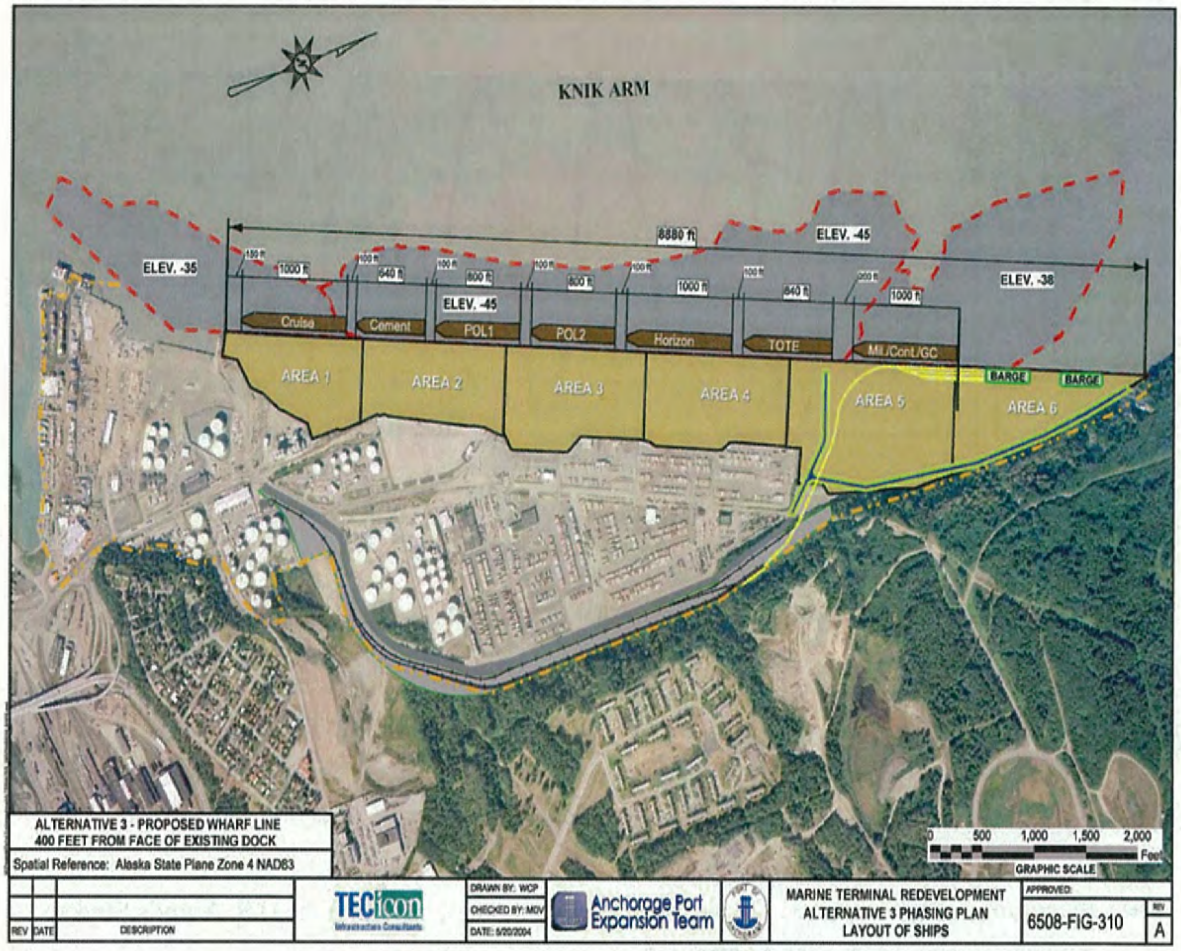

Figure 24. POA Expansion

The elevation of the ADCIRC grid nodes in the fill area were changed to 20 m above MSL, as shown in Figure 25. The linearity of the represented fill line was a function of the resolution of the ADCIRC grid. Depths in the harbor basin were assumed to be the same as they are presently, and they were unaltered from the exiting conditions (no additional dredging was reflected in the model topography).

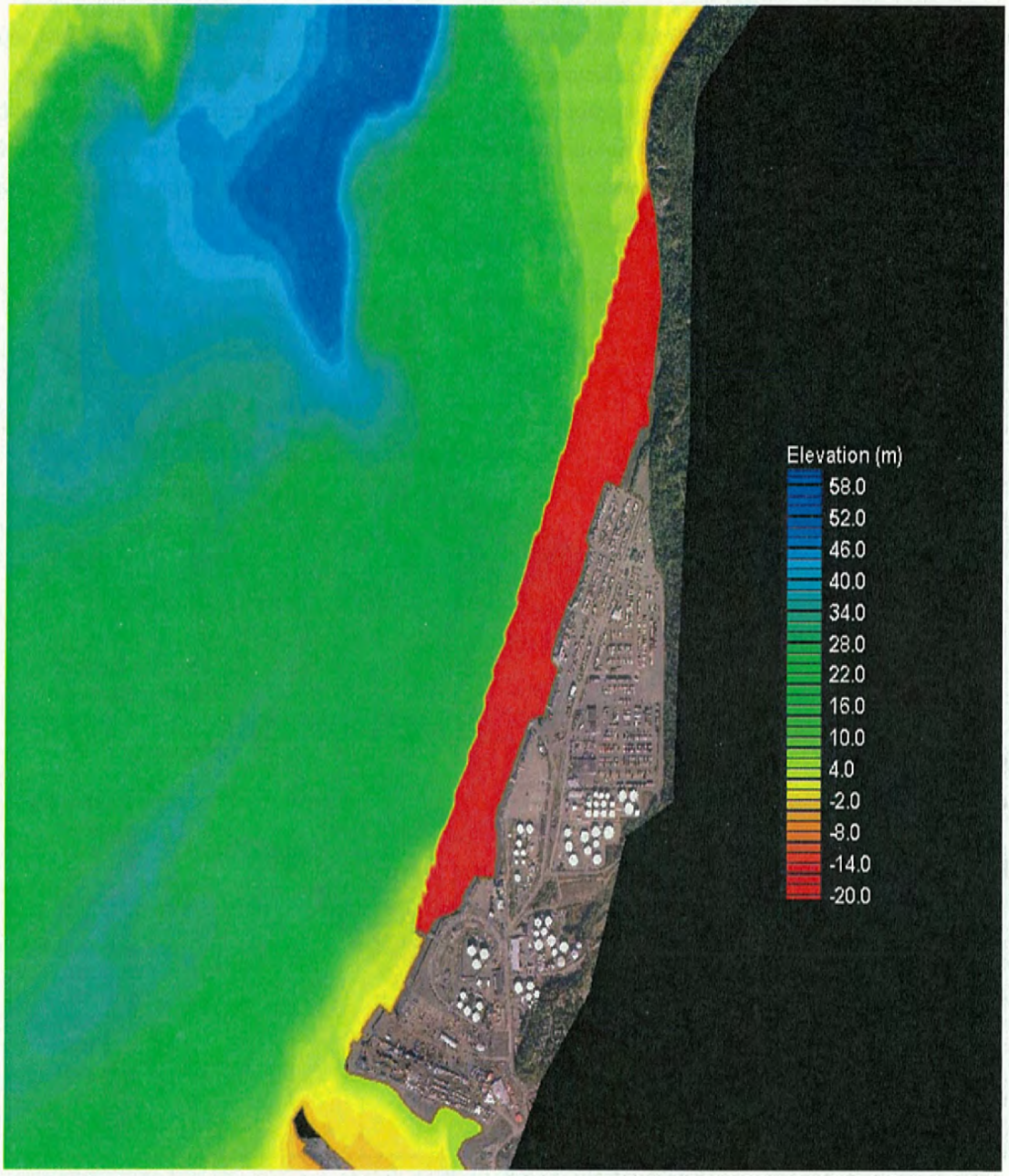

Figure 25 Fill Area in ADCIRC Grid

Hydrodynamic Influence of Proposed Expansion

Figure 26 shows the seventeen locations in the study area where comparisons of water level and current velocity were made, with and without the expansion. Locations at the existing and proposed dock face were produced to provide information about changes to current speeds at the proposed dock, compared to conditions that exist for the existing port configuration. Model results were also saved at several

locations along the tidelands which front wetlands south of the Port, at the entrance to the creek just south of the port, and at the entrance to Port MacKenzie, which is on the other side of Cook Inlet, to address concerns about the impact of the port expansion at these locations. Note that the tidelands that are fed by the creek just to the south of the Port are not included in the model, so flow at this point primarily relfects tidal flow conditions at the seaward entrance to the creek. In Figure 26, the bottom topography is shown in the colored contours (water depths are in meters).

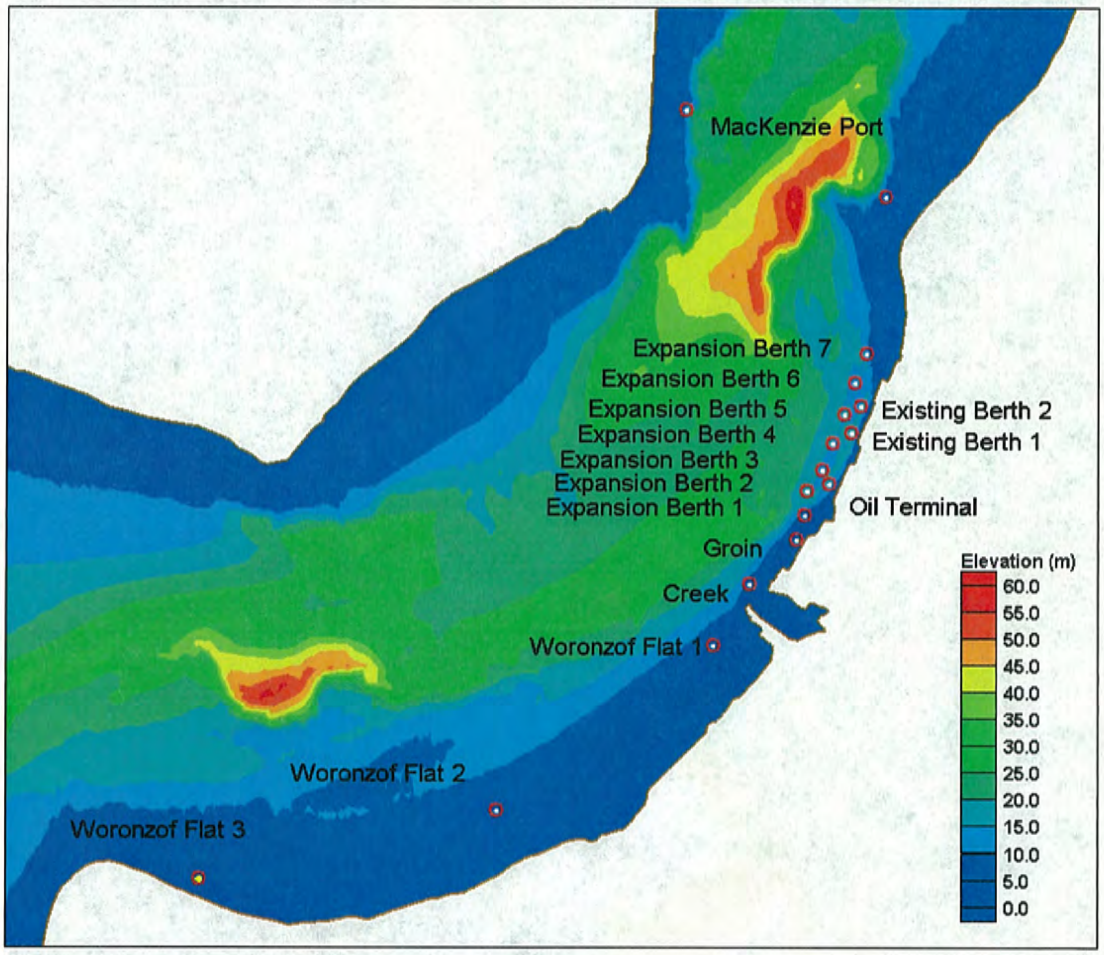

Figure 26 Stations for Water Level and Current Velocity Comparison

Figures 27 through 43 show time series of water level, during the simulation period at the seventeen stations, for with- and without-expansion conditions. The expansion fill covered the locations of three stations: Existing Berth 1, Existing Berth 2, and the figures for these locations. Some figures show very low values of water level (-99) which indicate that the station was dry during the corresponding time step.

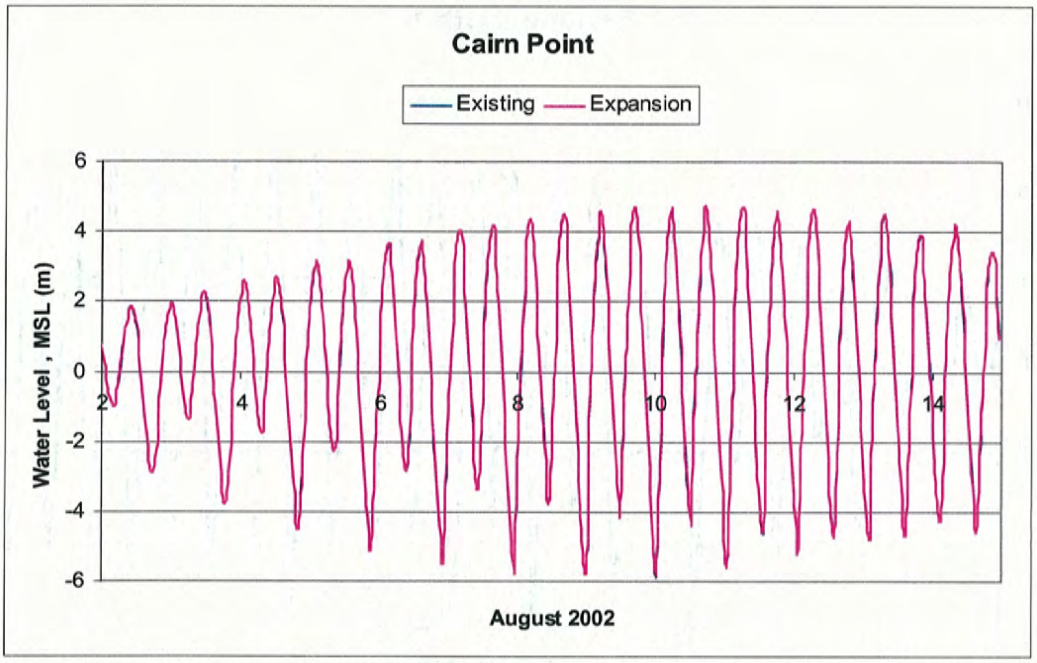

Figure 27 Time Series of Existing and with Expansion Water Level at Cairn Point

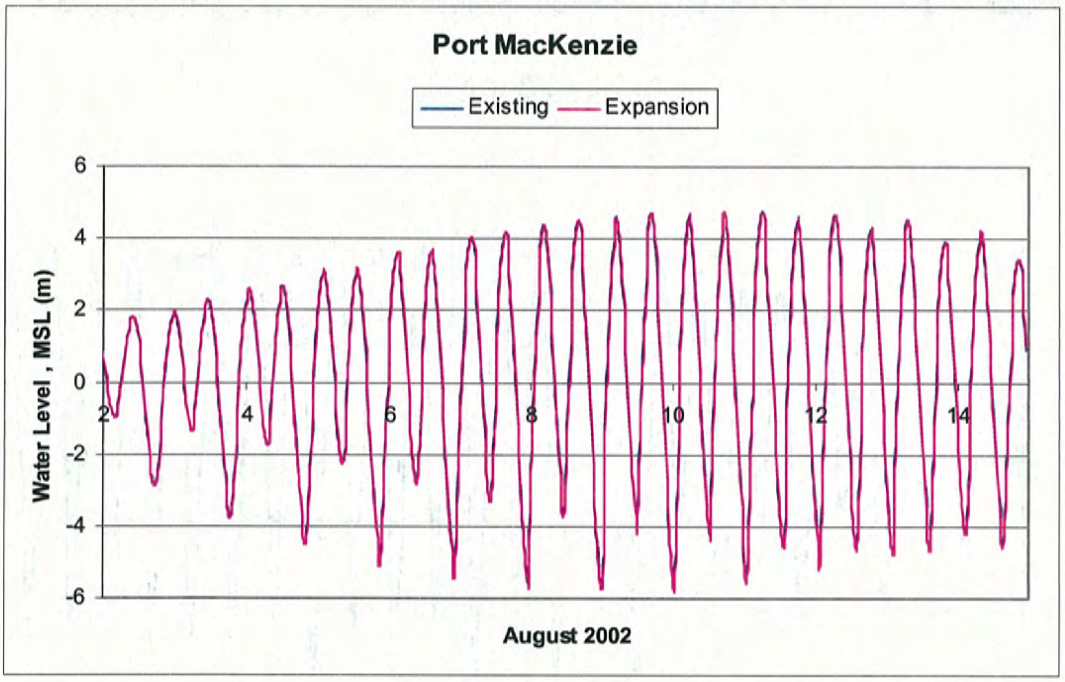

Figure 28 Time Series of Existing and with Expansion Water Level at Port MacKenzie

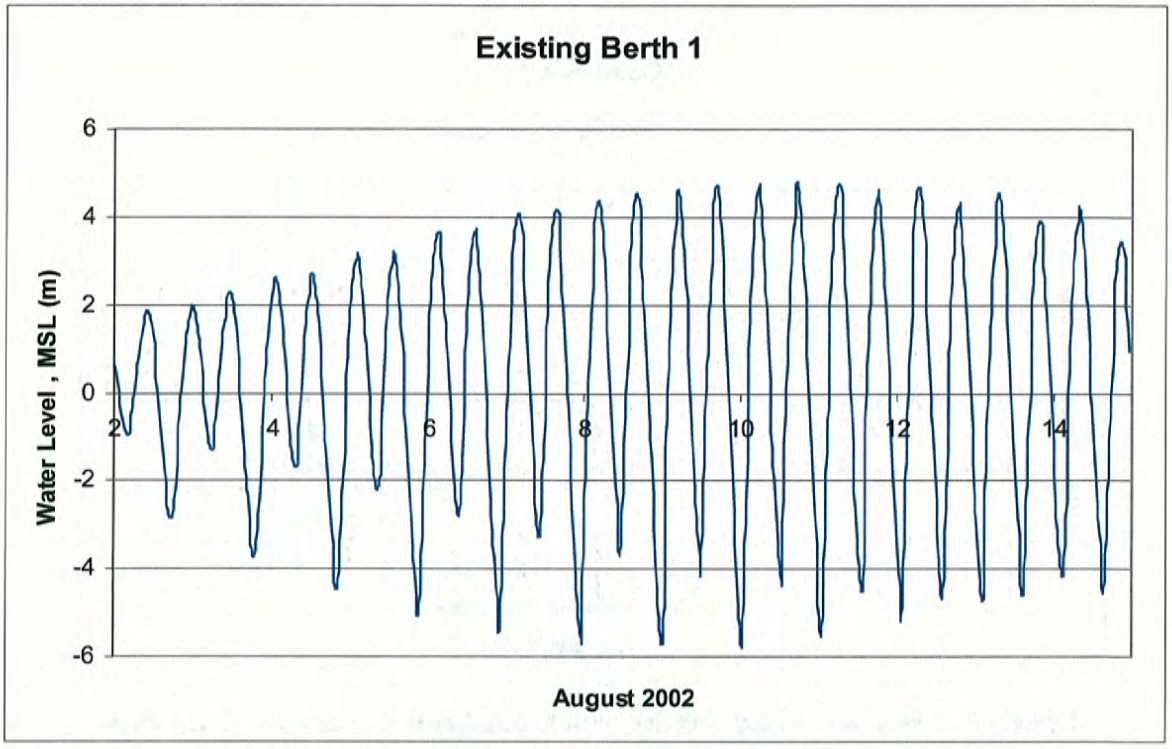

Figure 29 Time Series of Existing and with Expansion Water Level at Existing Berth 1

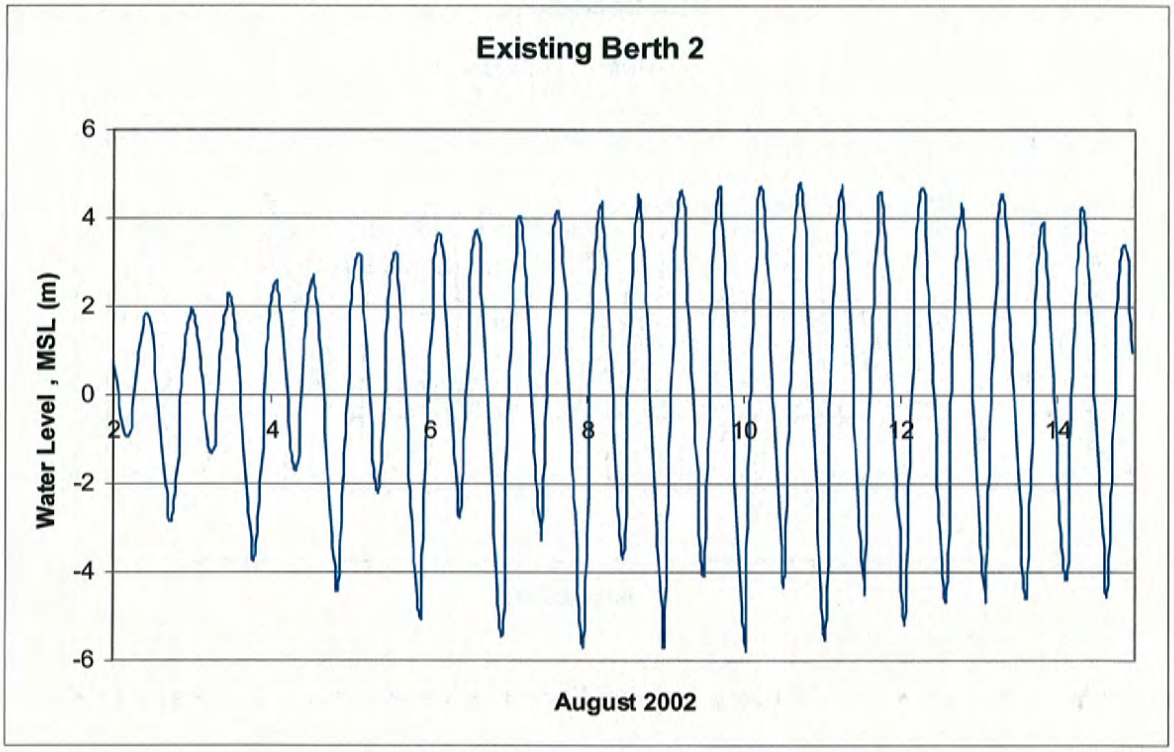

Figure 30 Time Series of Existing and with Expansion Water Level at Existing Berth 2

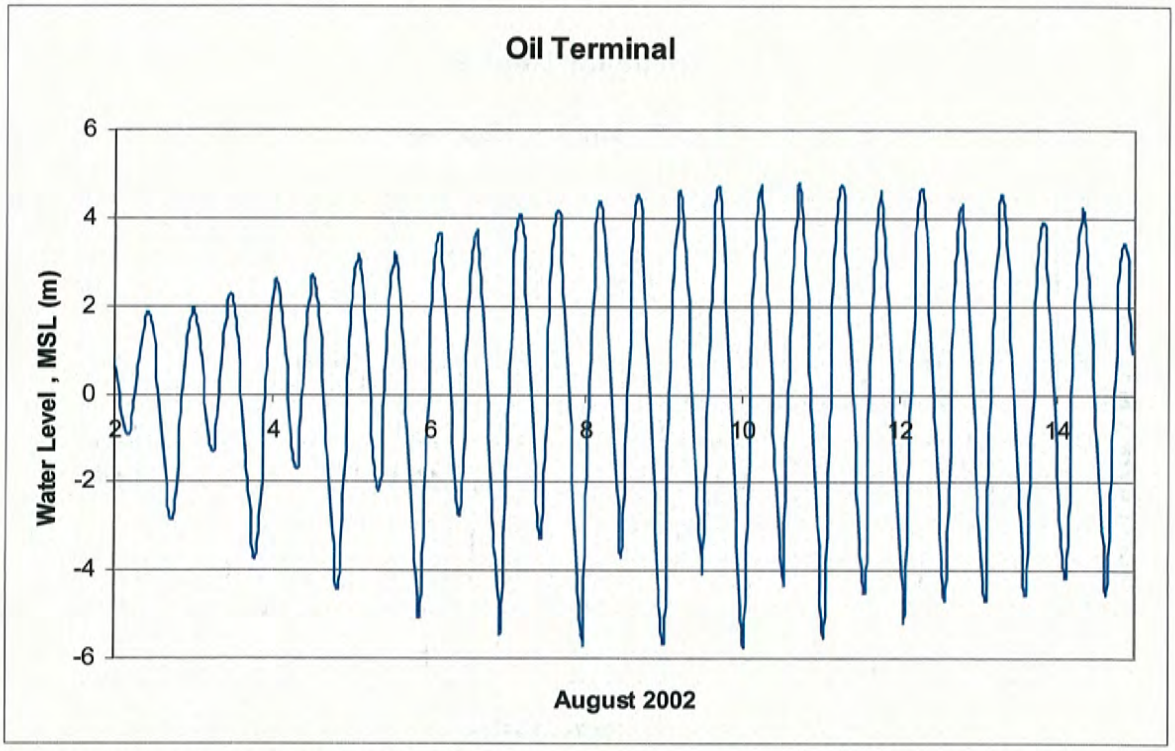

Figure 31 Time Series of Existing and with Expansion Water Level at Oil Terminal

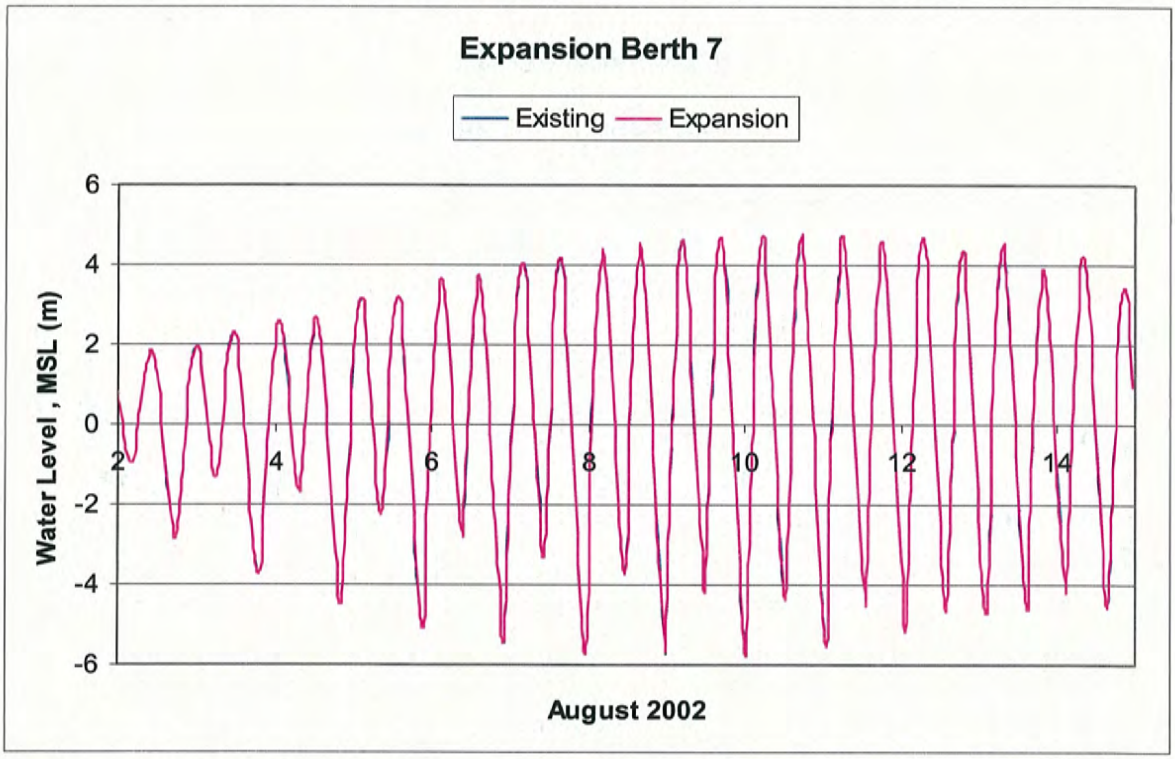

Figure 32 Time Series of Existing and with Expansion Water Level at Expansion Berth 7

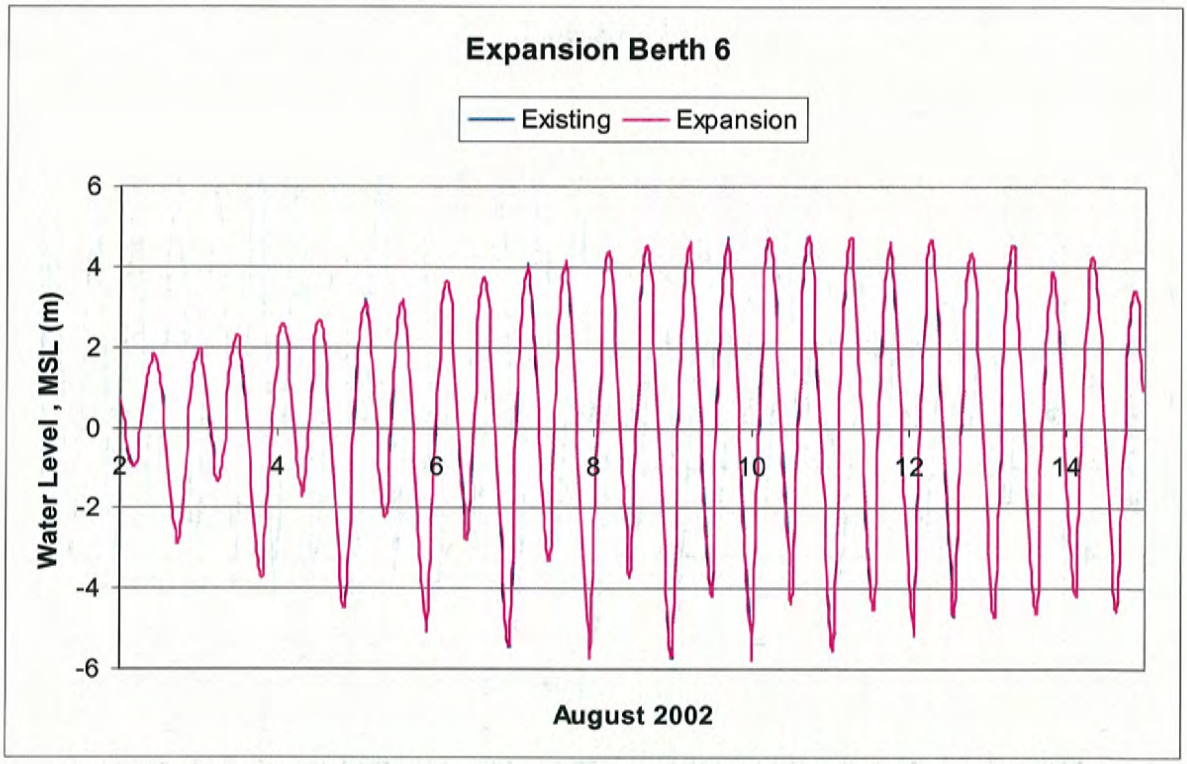

Figure 33 Time Series of Existing and with Expansion Water Level at Expansion Berth 6

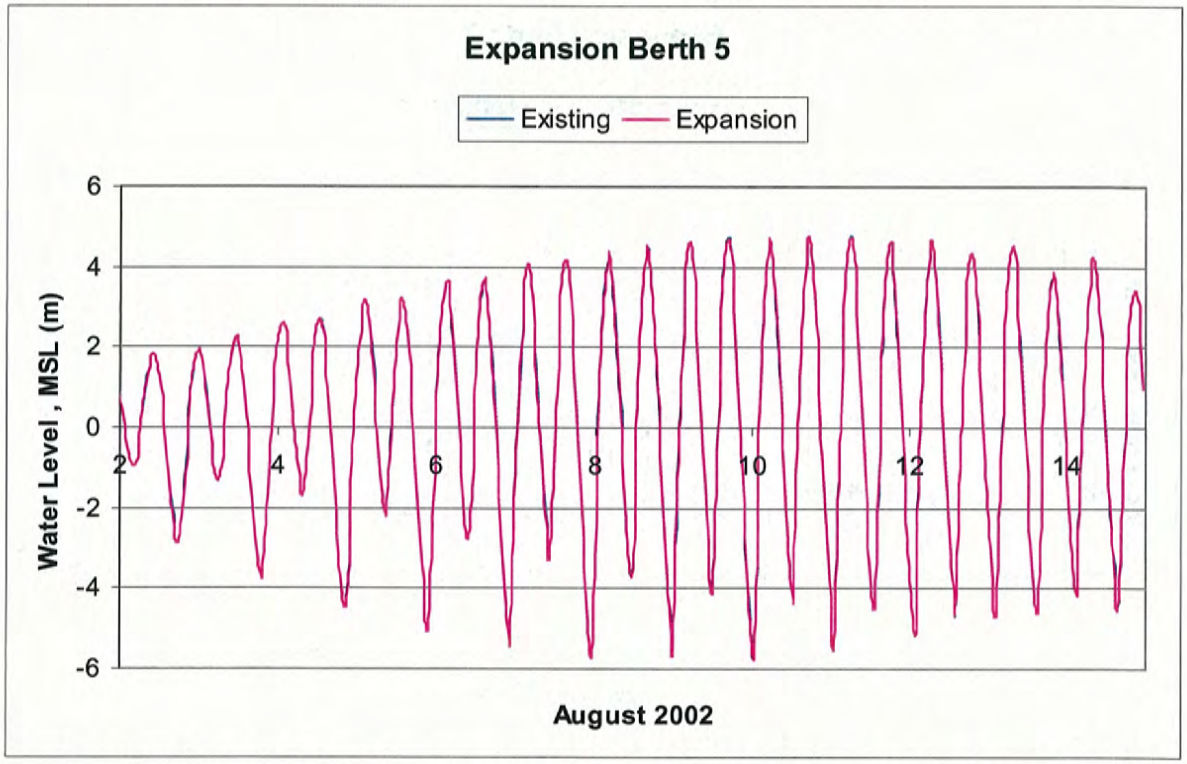

Figure 34 Time Series of Existing and with Expansion Water Level at Expansion Berth 5

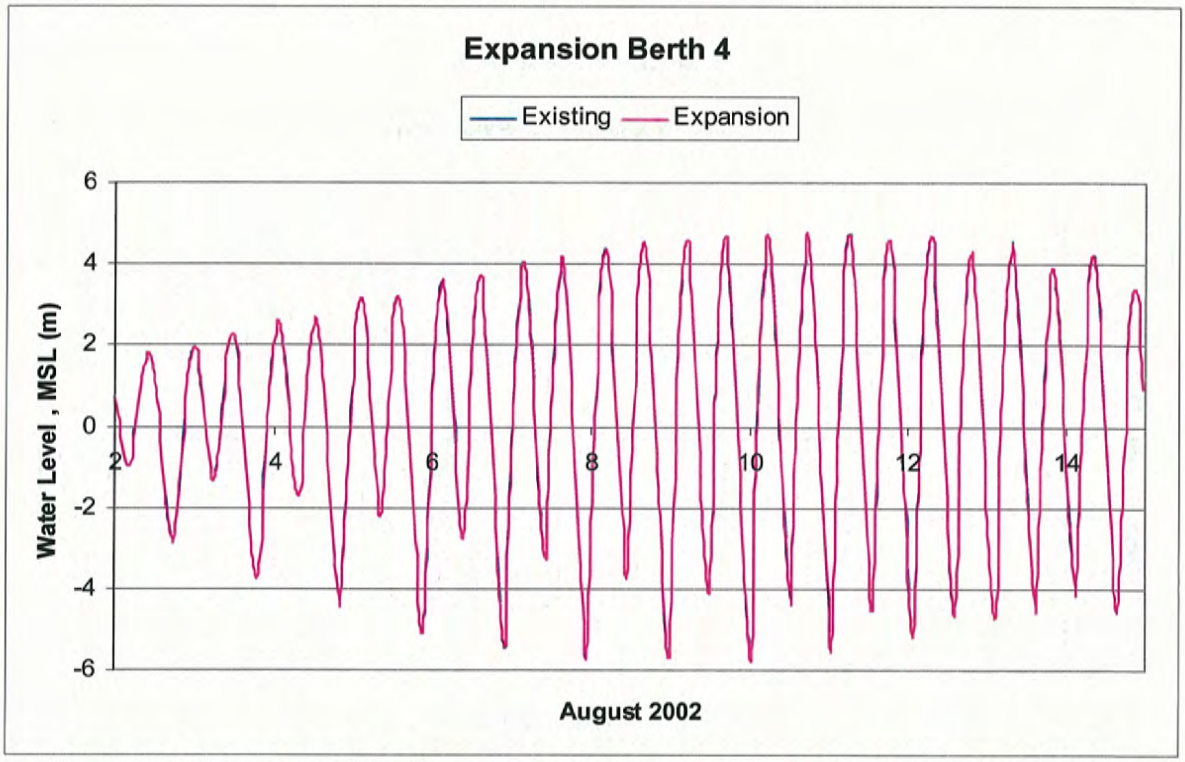

Figure 35 Time Series of Existing and with Expansion Water Level at Expansion Berth 4

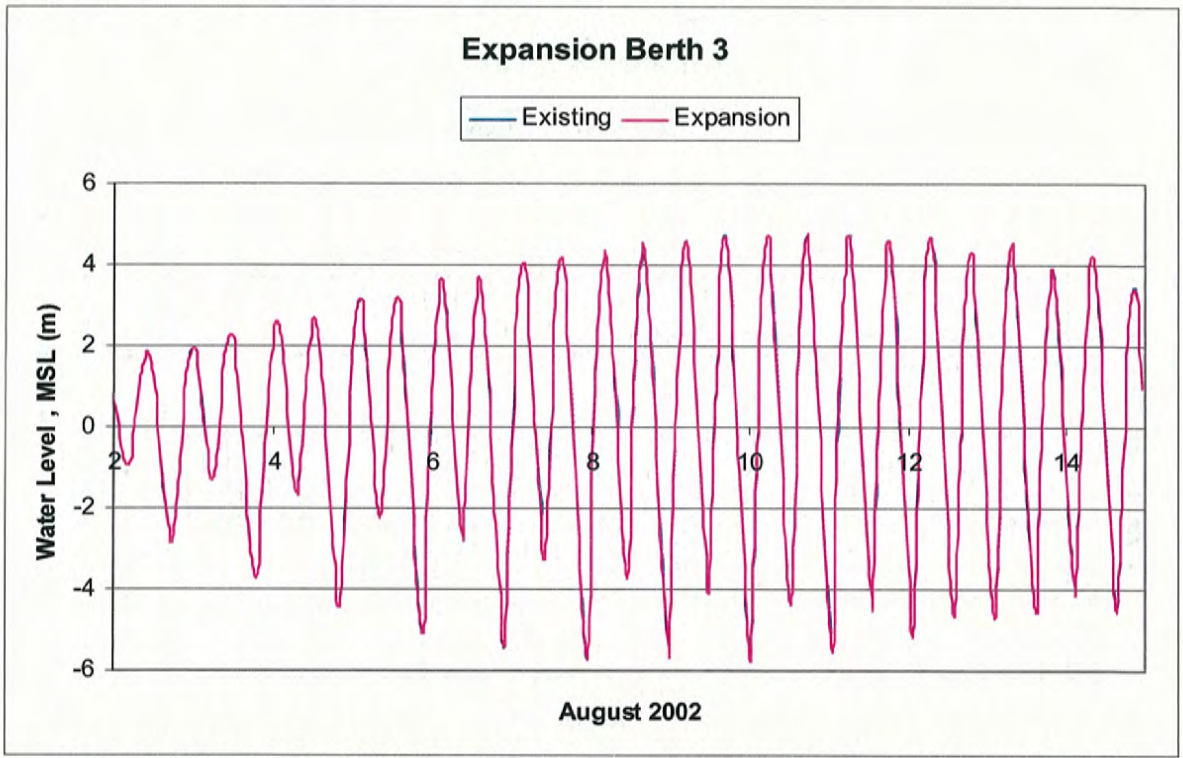

Figure 36 Time Series of Existing and with Expansion Water Level at Expansion Berth 3

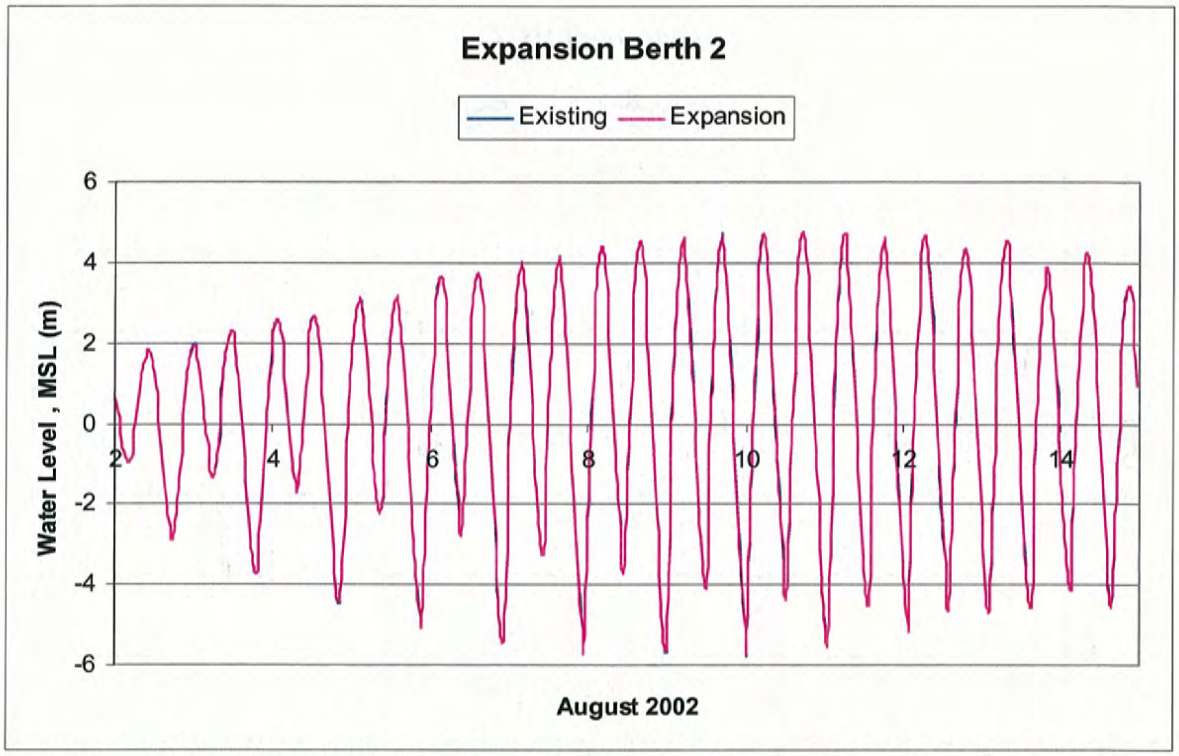

Figure 37 Time Series of Existing and with Expansion Water Level at Expansion Berth 2

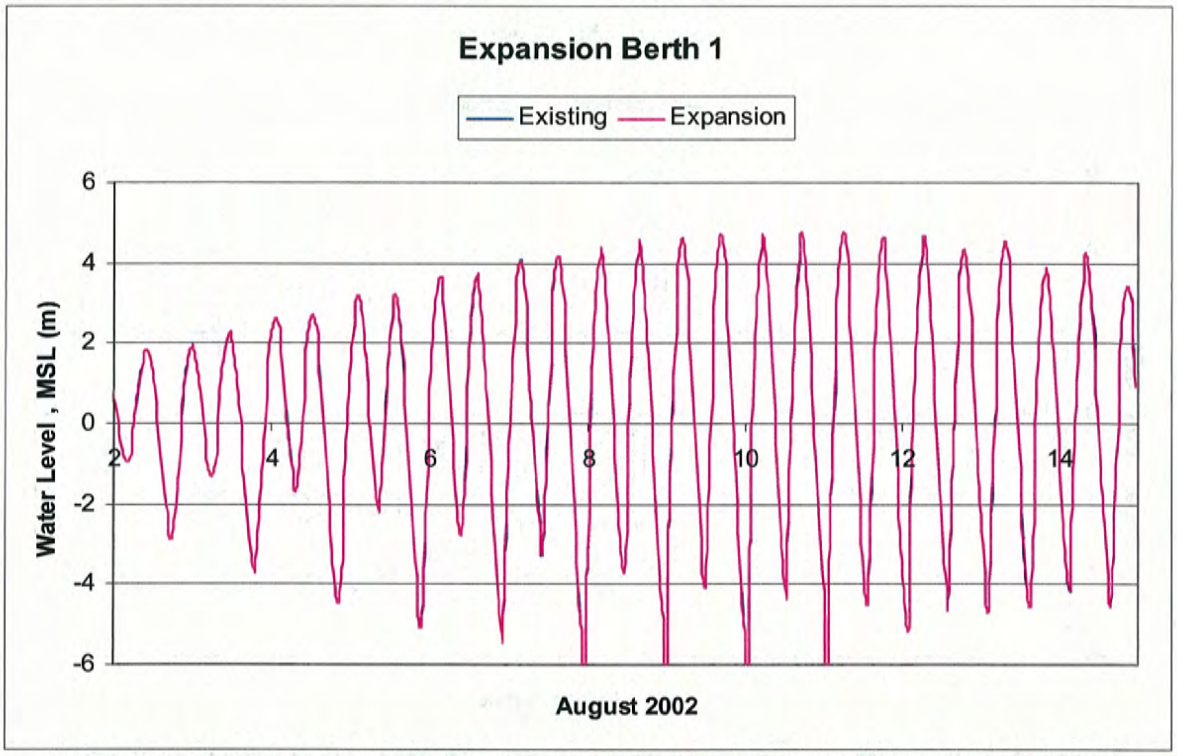

Figure 38 Time Series of Existing and with Expansion Water Level at Expansion Berth 1

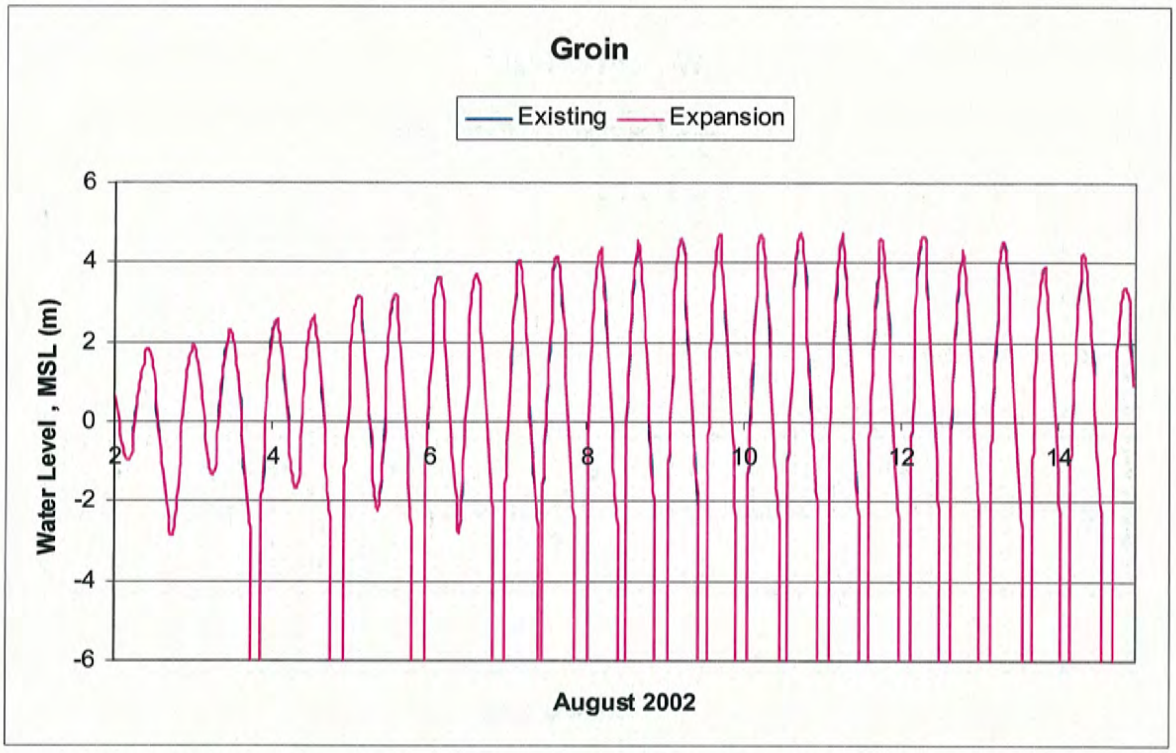

Figure 39 Time Series of Existing and with Expansion Water Level at the Groin

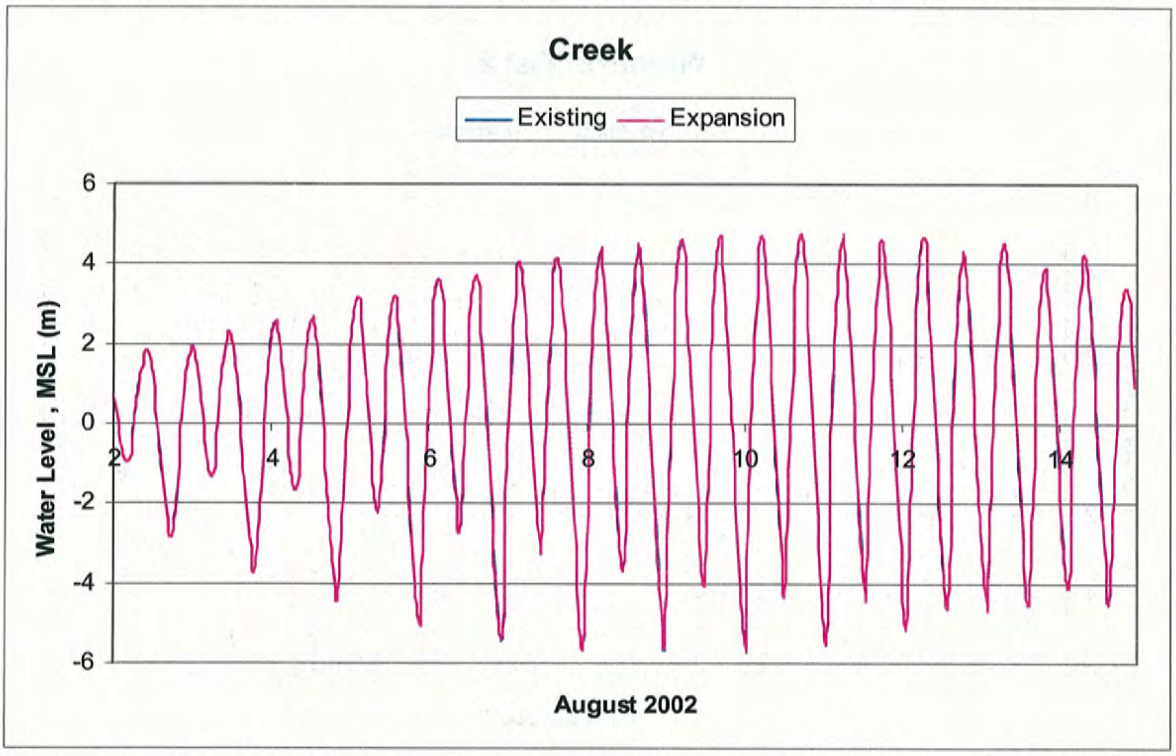

Figure 40 Time Series of Existing and with Expansion Water Level at the Creek

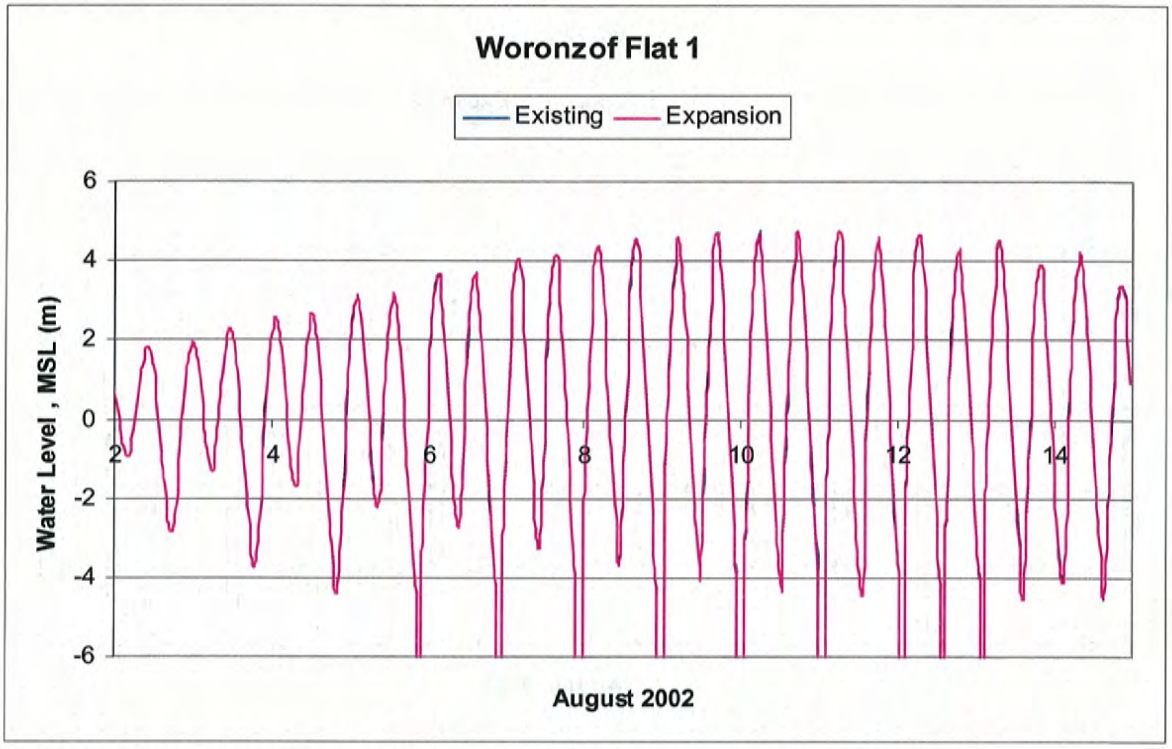

Figure 41 Time Series of Existing and with Expansion Water Level at Woronzof Flat 1

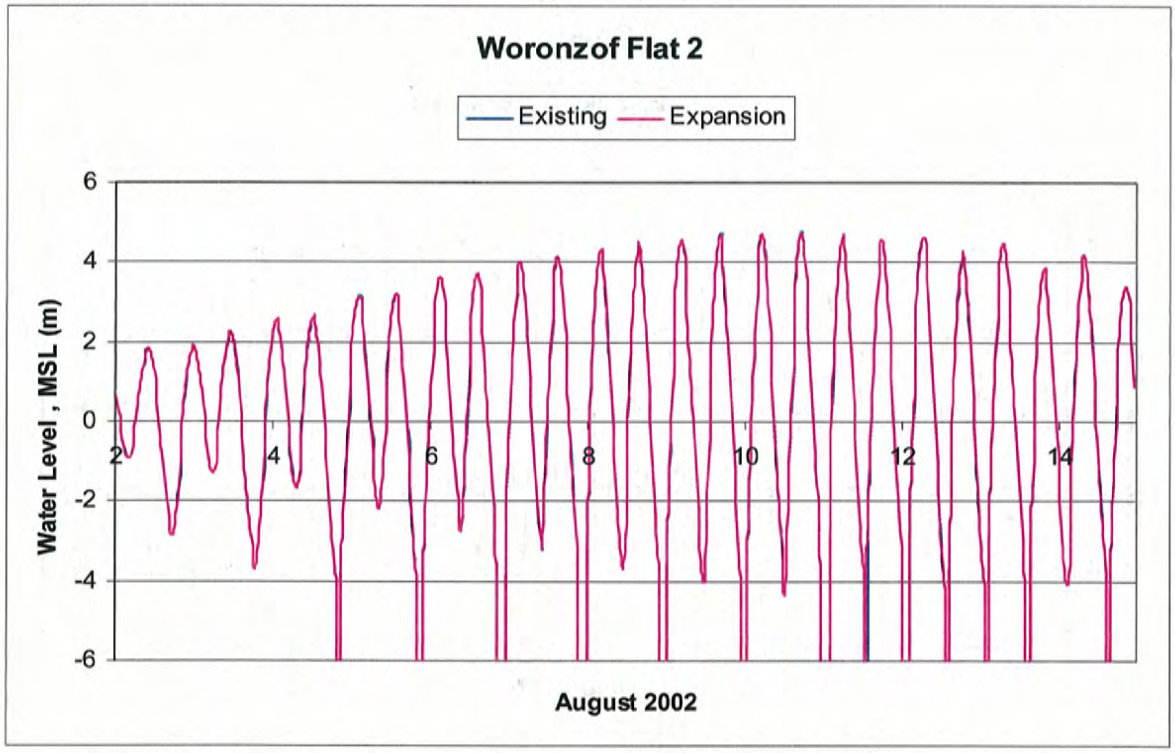

Figure 42 Time Series of Existing and with Expansion Water Level at Woronzof Flat 2

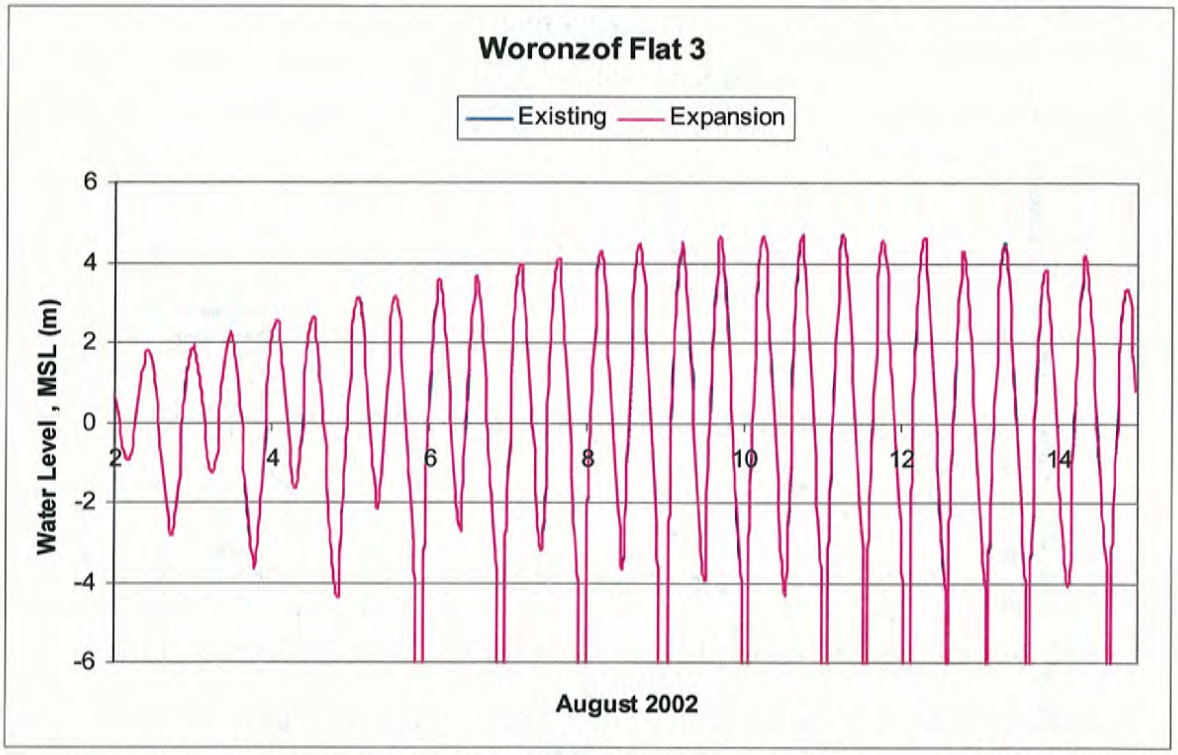

Figure 43 Time Series of Existing and with Expansion Water Level at Woronzof Flat 3

Results are shown for the full spring-neap tidal cycle (some time at the beginning was model spin up time). As expected, the expansion did not change the water level in the area. The proposed expansion has no effect on the water level at the Port or the propagation of the tide wave through upper Cook Inlet.

Figures 44 through 57 show time series of current speed and direction, during the complete spring-neap simulation period, at fourteen stations before and after the expansion (the three stations at the existing dock face, which are not relevant for the expansion, were not plotted). The figures also show the water level at Anchorage NOAA station. Figures 58 through 65 show time series of current speed and direction, during two days of the spring tide, at the seven Expansion Berth stations and at the Creek station, with and without the expansion.

It can be seen from Figure 44 that at Cairn Point the current structure is changed very little during the entire spring-neap cycle (in terms of both speed and direction). Current speed during flood flow is increased slightly during neap tide conditions, with the expansion in place. During spring tide conditions, changes are even less. Overall, at this location near Cairn Point, changes in velocity are negligible. Other graphical products presented later show the same basic result. At Port MacKenzie, change in current speed and direction are unaffected by the proposed expansion (seen in Figure 45).

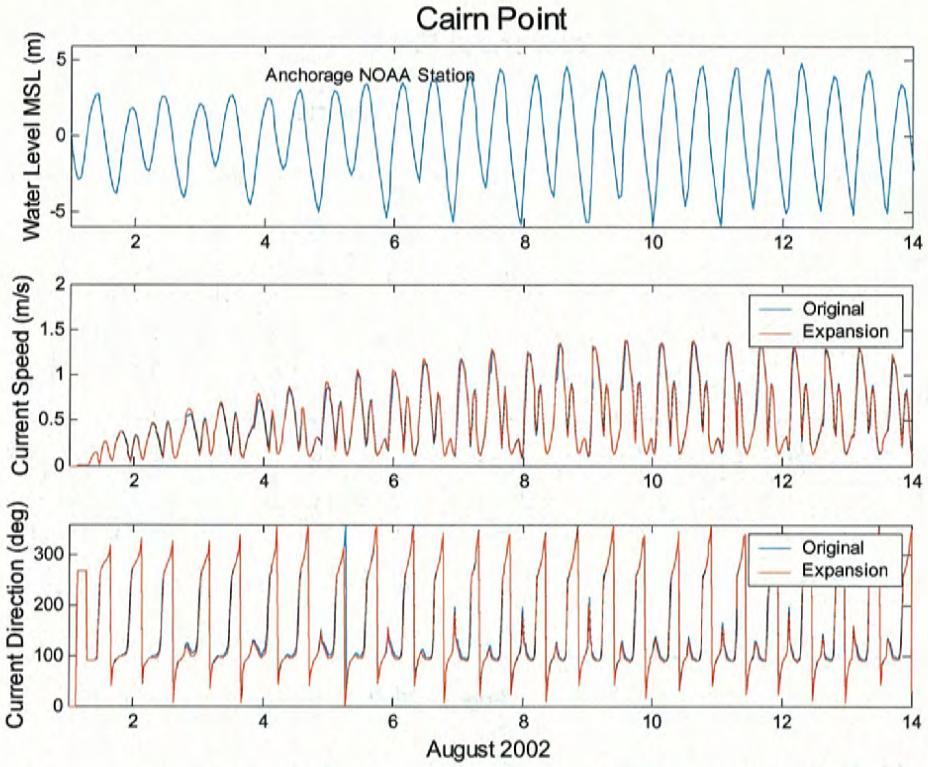

Figure 44 Time series of Existing and with Expansion Current Speed and Direction at Cairn Point

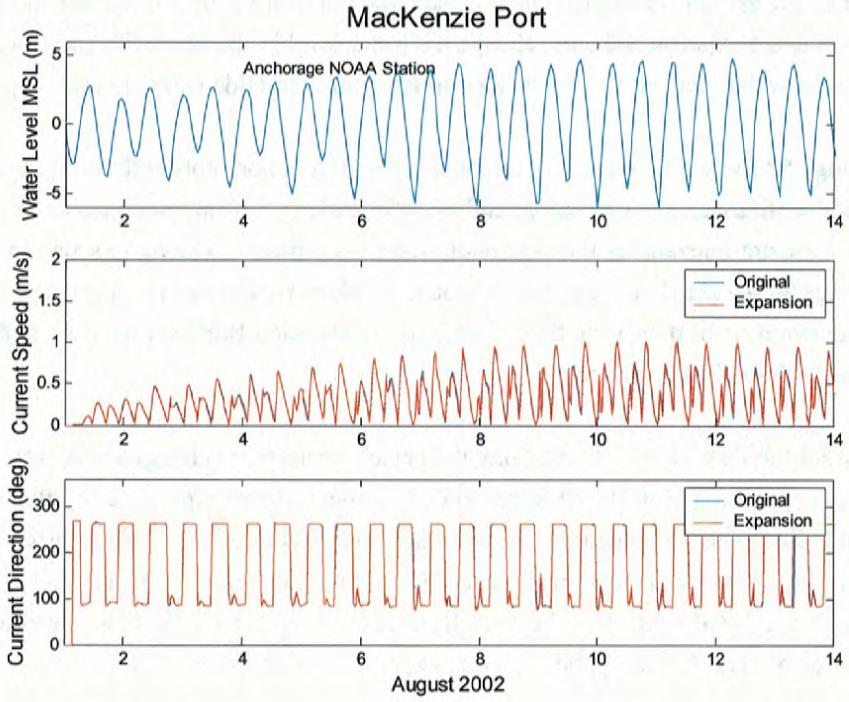

Figure 45 Time Series of Existing and with Expansion Currents at Port MacKenzie

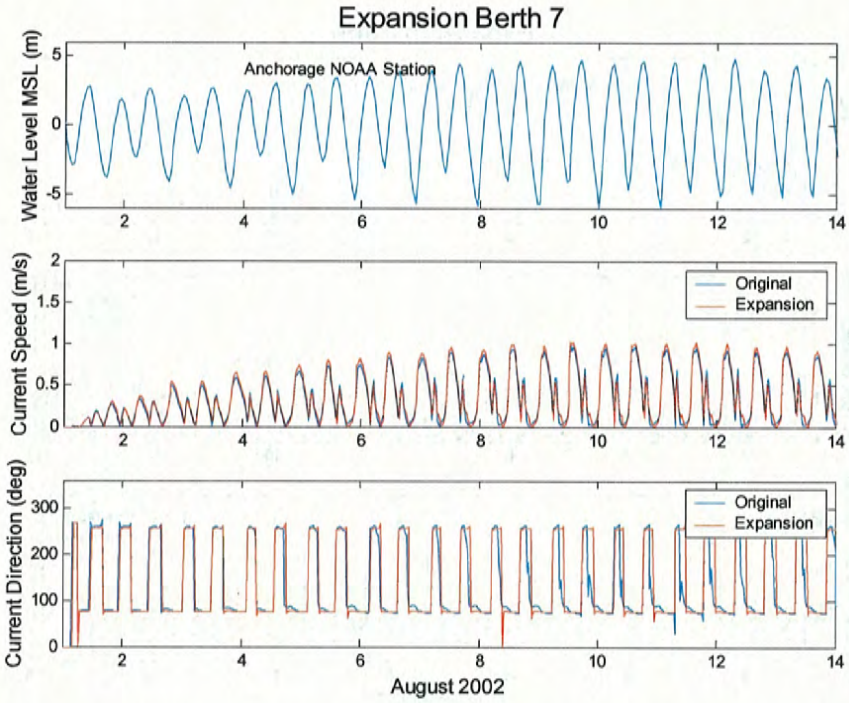

Figure 46 Time Series of Existing and with Expansion Current Speed and Direction at Expansion Berth 7

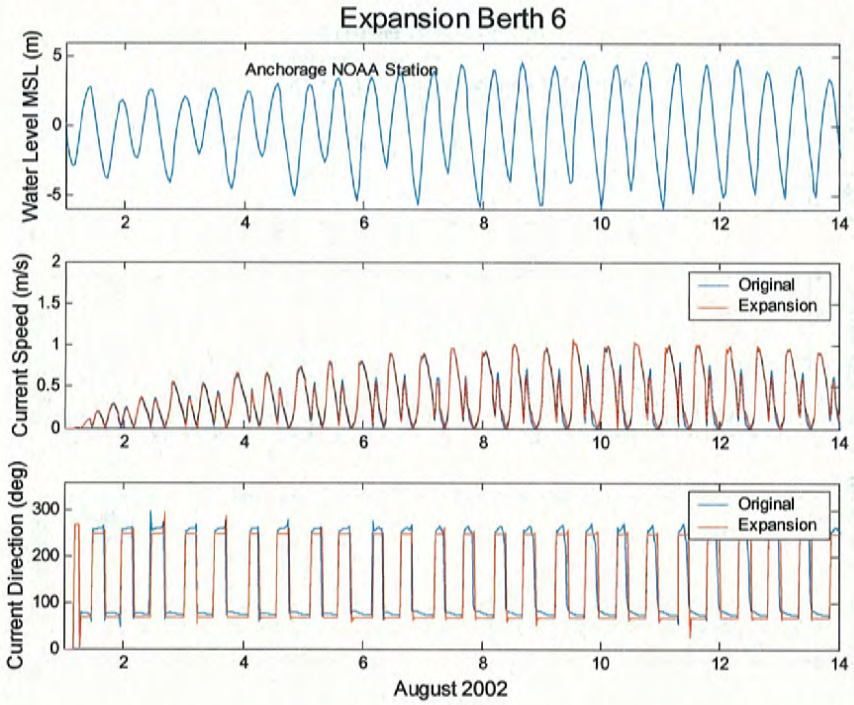

Figure 47. Time Series of Existing and with Expansion Current Speed and Direction at Expansion Berth 6

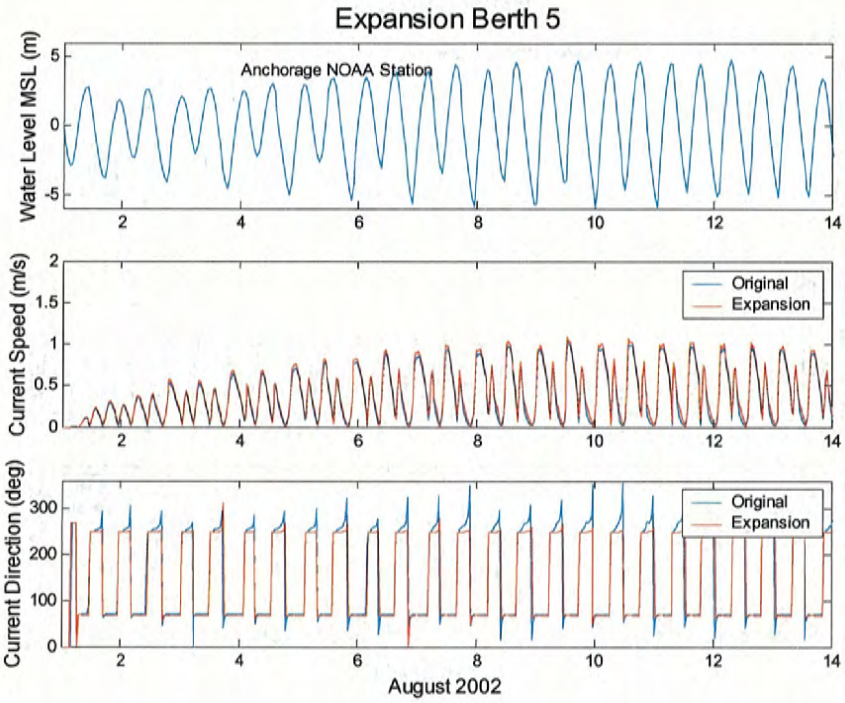

Figure 48 Time Series of Existing and with Expansion Current Speed and Direction at Expansion Berth 5

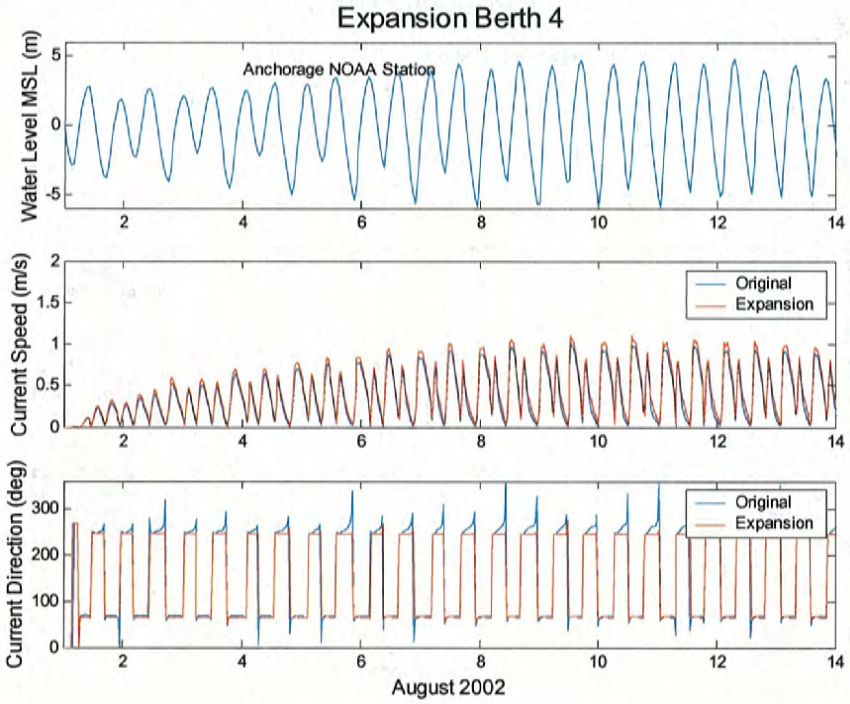

Figure 49 Time Series of Existing and with Expansion Current Speed and Direction at Expansion Berth 4

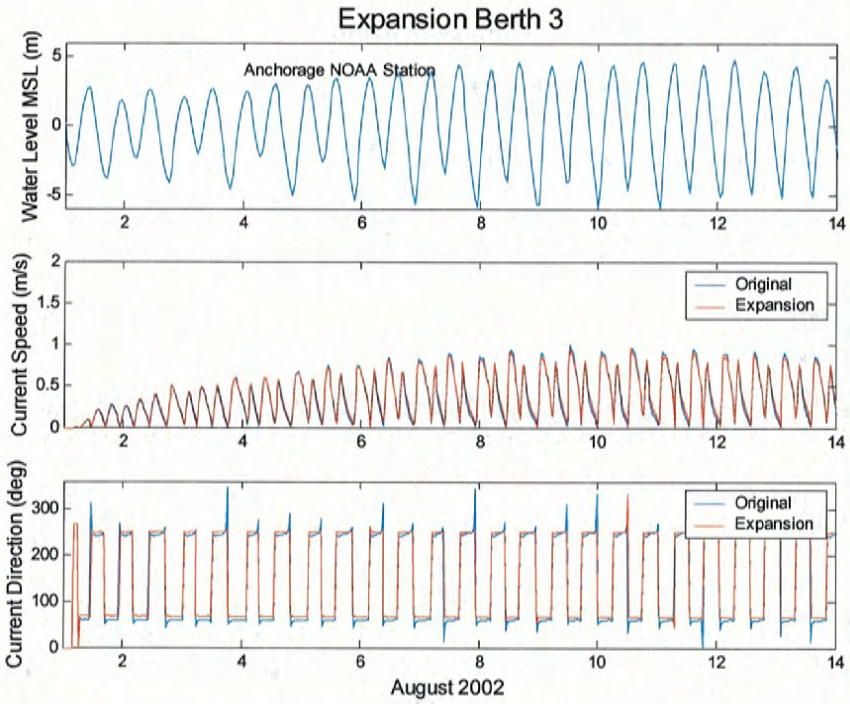

Figure 50 Time Series of Existing and with Expansion Current Speed and Direction at Expansion Berth 3

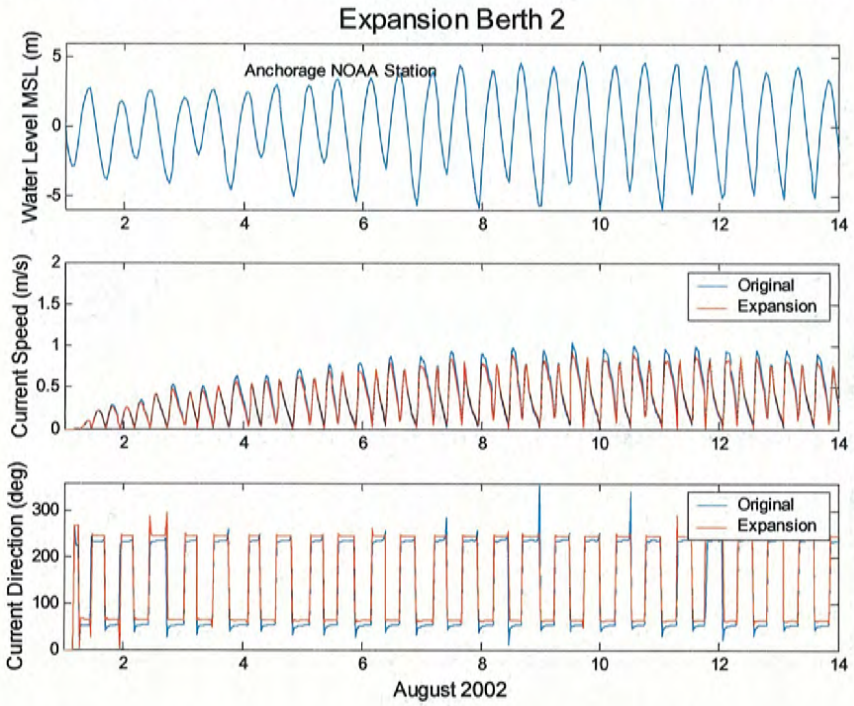

Figure 51 Time Series of Existing and with Expansion Current Speed and Direction at Expansion Berth 2

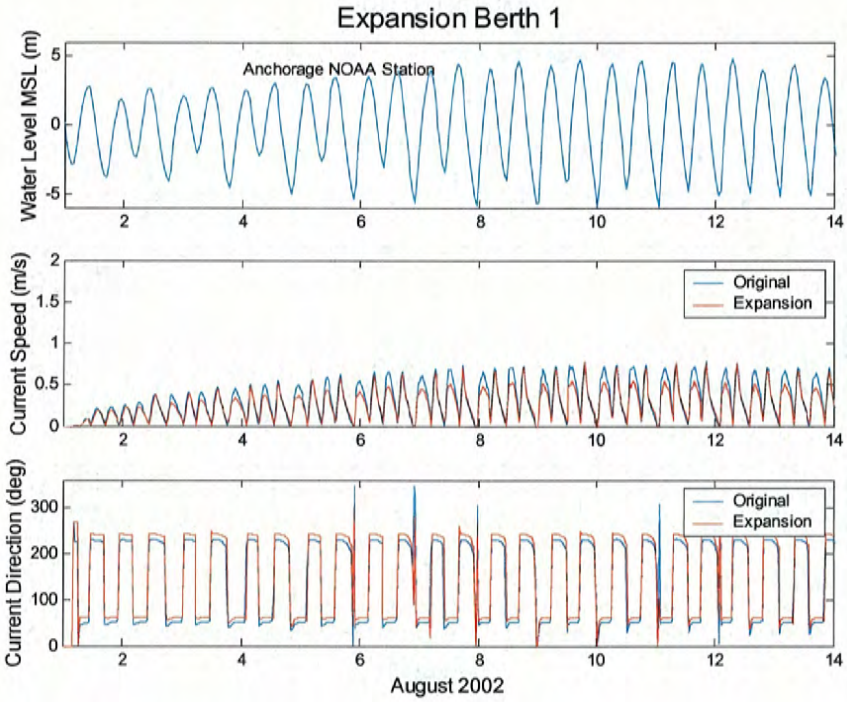

Figure 52 Time Series of Existing and with Expansion Current Speed and Direction at Expansion Berth 1

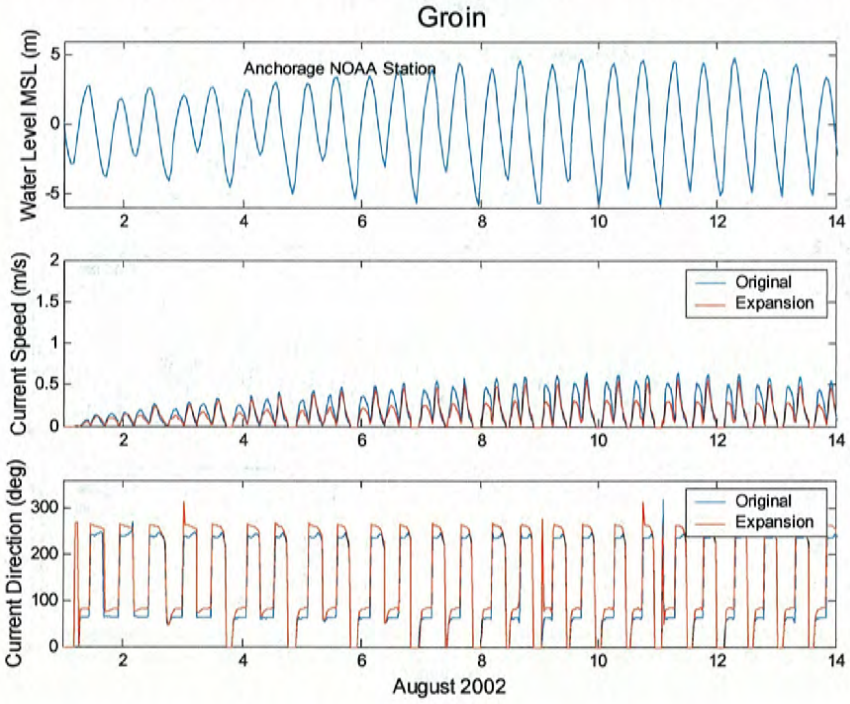

Figure 53 Time Series of Existing and with Expansion Current Speed and Direction at the Groin

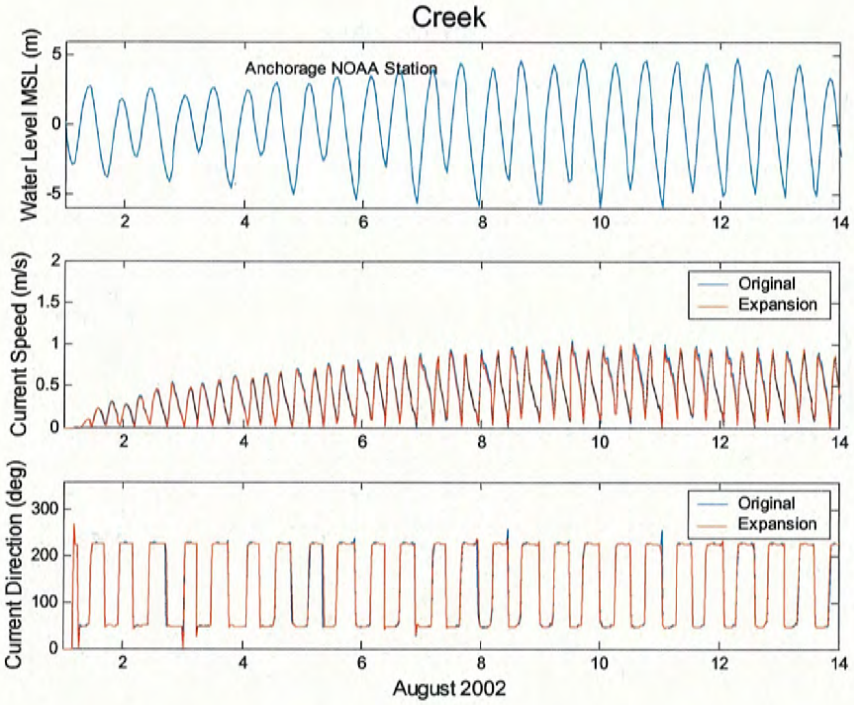

Figure 54 Time Series of Existing and with Expansion Current Speed and Direction at the Creek

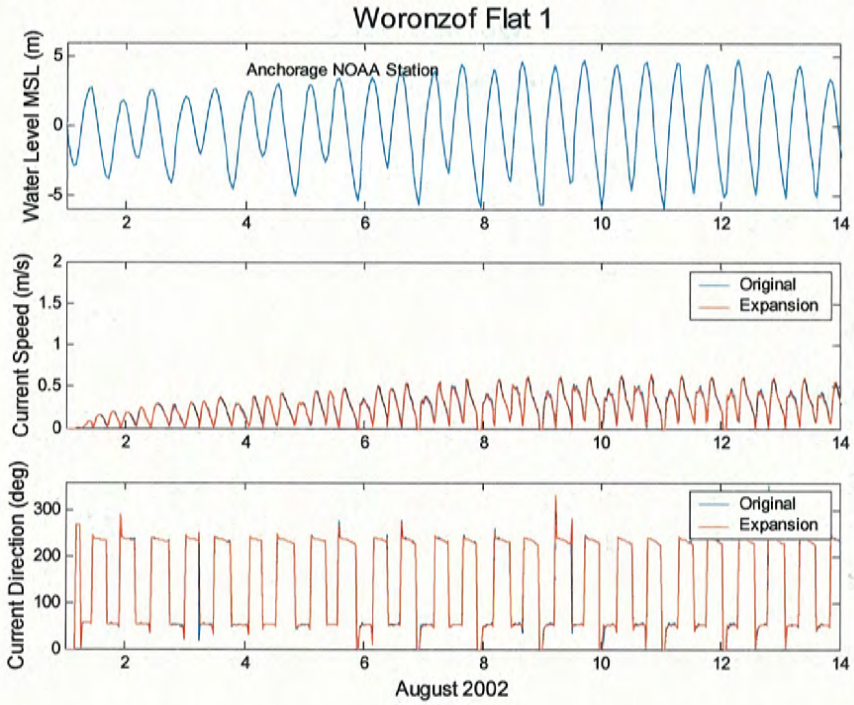

Figure 55 Time Series of Existing and with Expansion Current Speed and Direction at Woronzof Flat 1

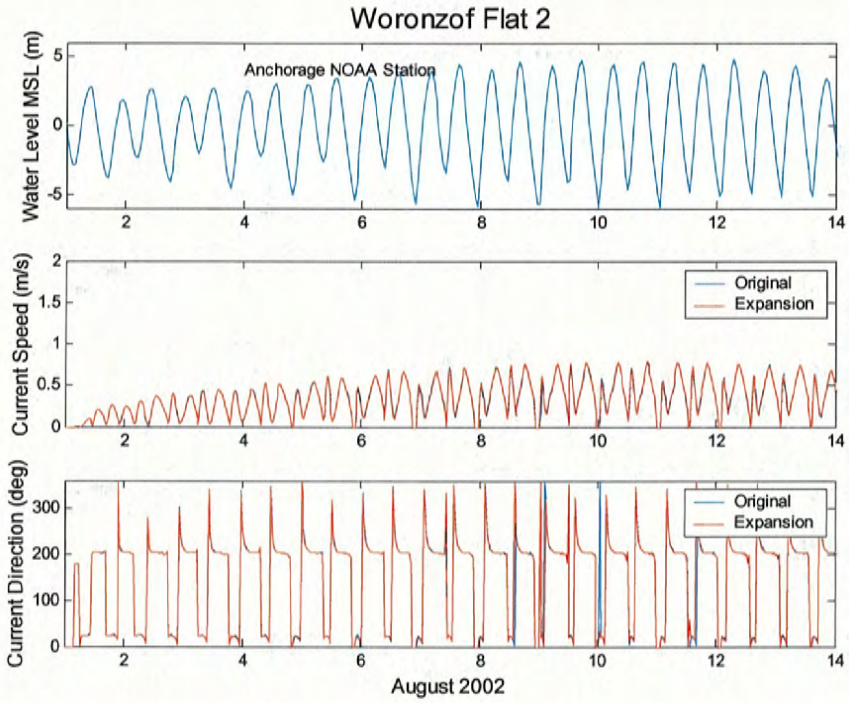

Figure 56 Time Series of Existing and with Expansion Current Speed and Direction at Woronzof Flat 2

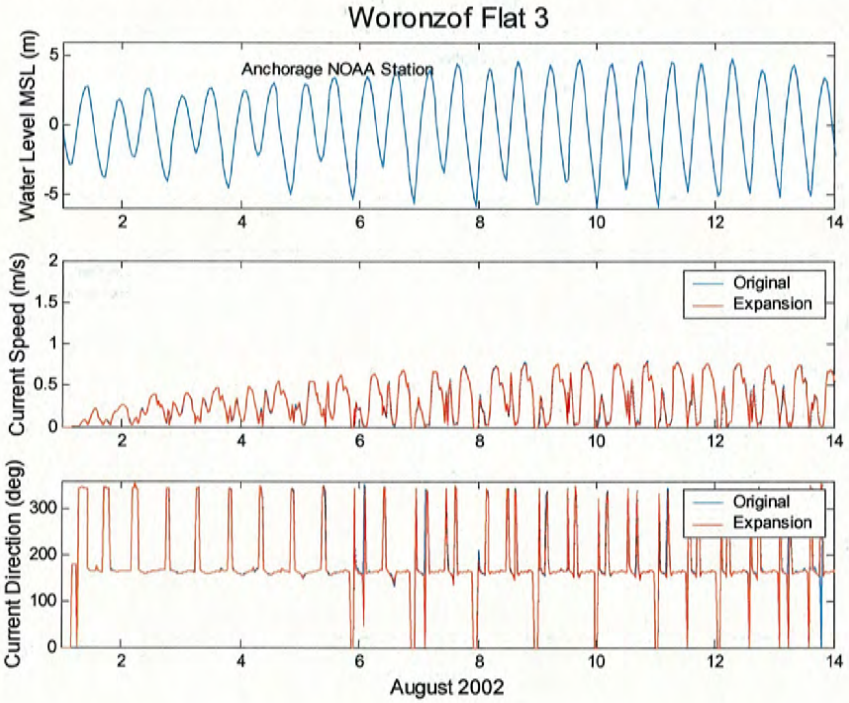

Figure 57 Time Series of Existing and with Expansion Current Speed and Direction at Woronzof Flat 3

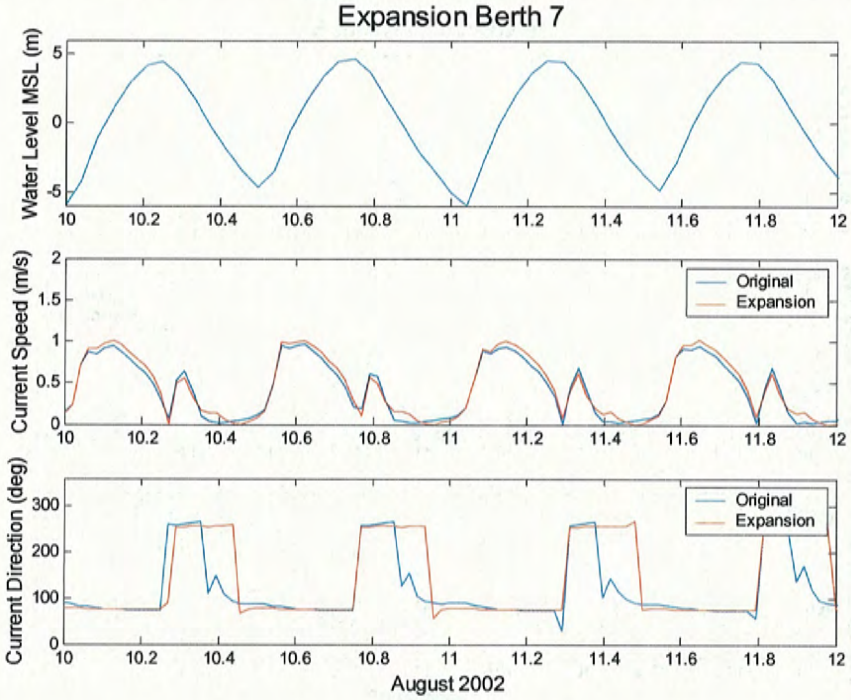

Figure 58 Time Series of Existing and with Expansion Current Speed and Direction at Expansion Berth 7 During Spring Tide

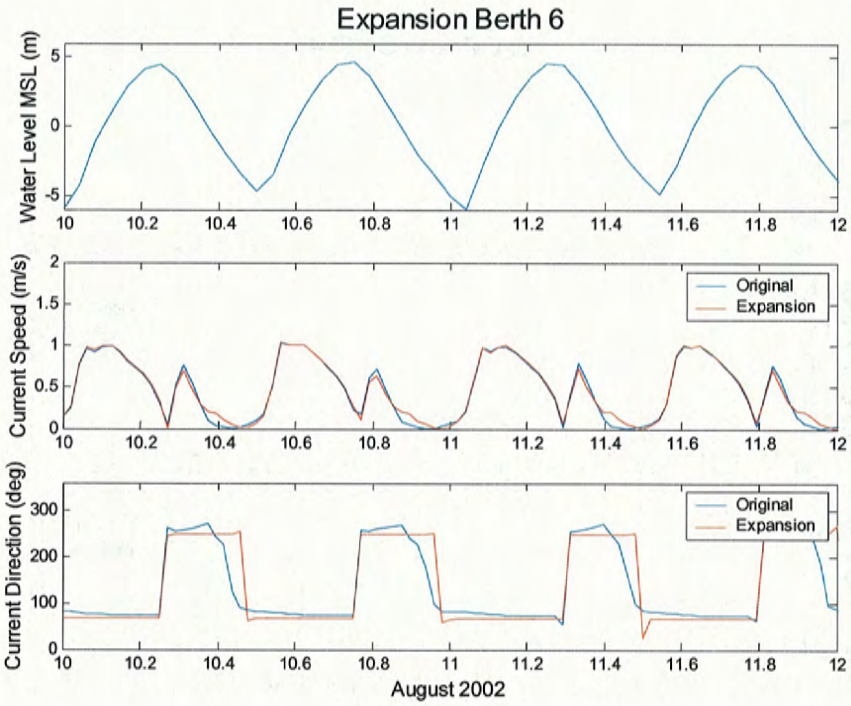

Figure 59. Time Series of Existing and with Expansion Current Speed and Direction at Expansion Berth 6 During Spring Tide

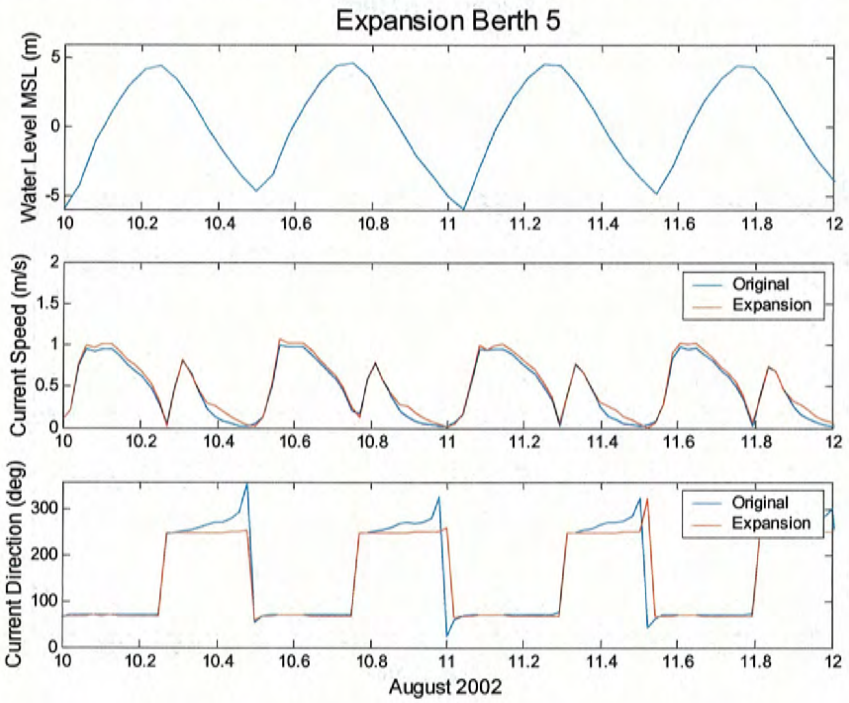

Figure 60 Time Series of Existing and with Expansion Current Speed and Direction at Expansion Berth 5 During Spring Tide

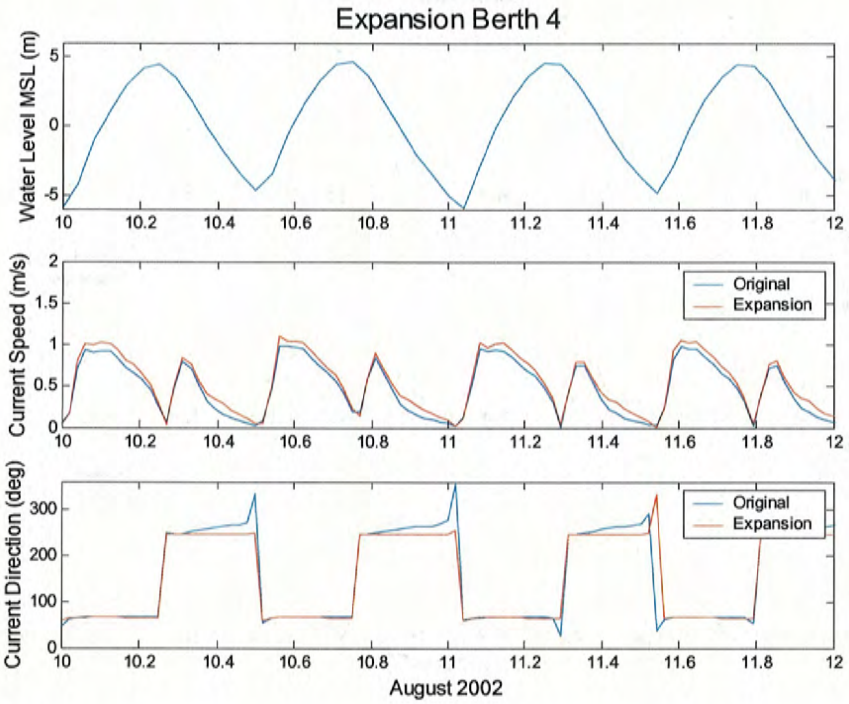

Figure 61 Time Series of Existing and with Expansion Current Speed and Direction at Expansion Berth 4 During Spring Tide

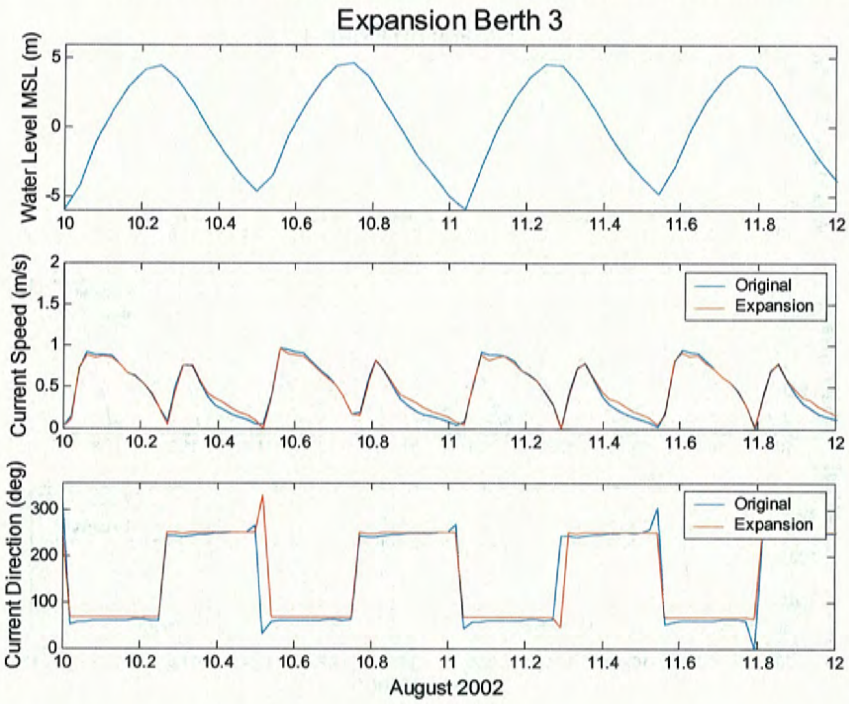

Figure 62 Time Series of Existing and with Expansion Current Speed and Direction at Expansion Berth 3 During Spring Tide

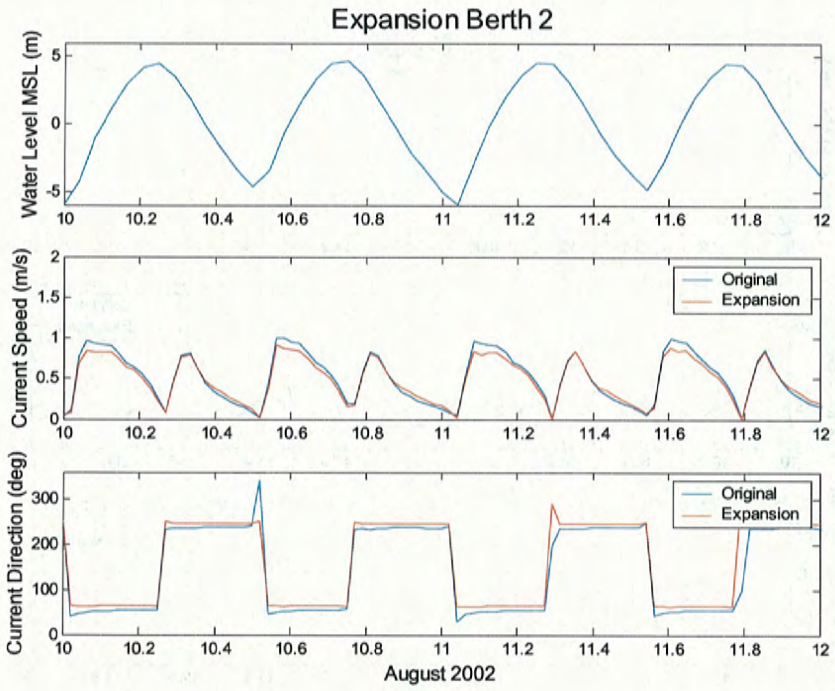

Figure 63 Time Series of Existing and with Expansion Current Speed and Direction at Expansion Berth 2 During Spring Tide

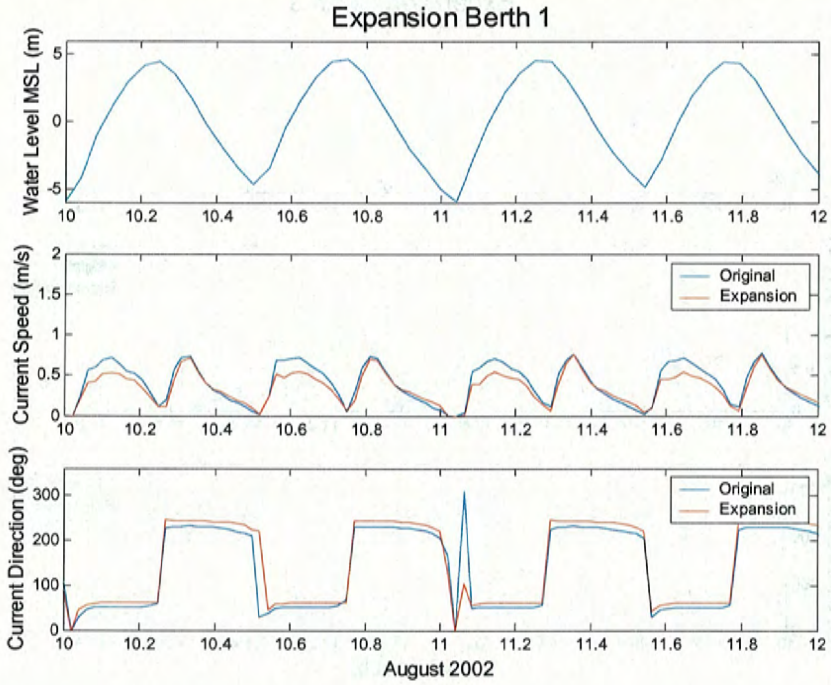

Figure 64 Time Series of Existing and with Expansion Current Speed and Direction at Expansion Berth 1 During Spring Tide

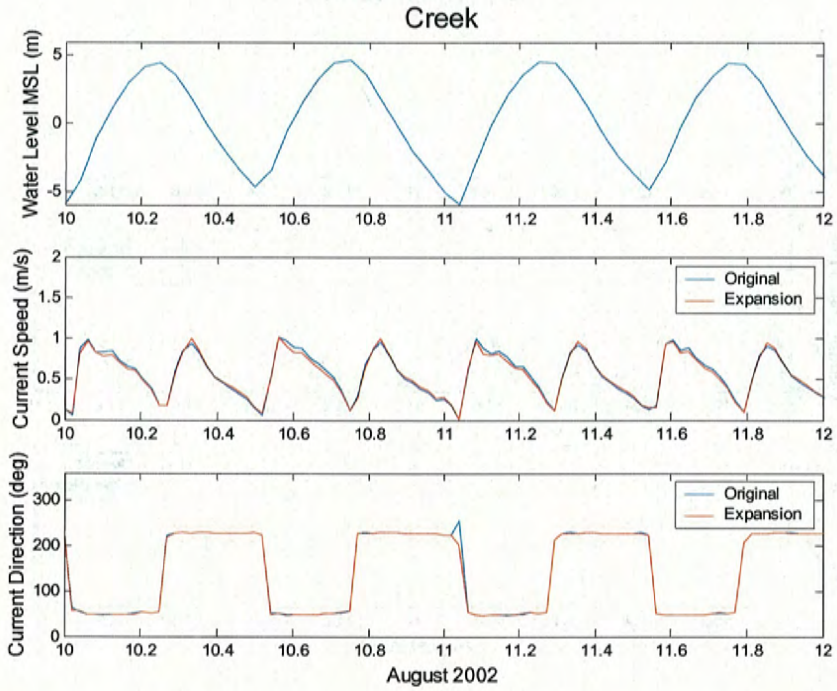

Figure 65 Time Series of Existing and with Expansion Current Speed and Direction at the Creek During Spring Tide

At Expansion Berth 7 station, Figures 46 and 58 show that the current speed on flood flow generally increased at this location with the expansion in place, but by only about 5 cm/sec (0.05 m/sec), a rather minor change. Peak spring flood currents at this location approach 1 m/sec, so the change is on the order of 5%. This slight increase was observed throughout the neap-spring cycle. During spring tide conditions, during the early stages of ebb flow, the expansion produced a slight decrease in ebb current strength, again about 5 cm/sec. In the later stages of the spring ebb cycle, the expansion changed the character of the tide at this location. An eddy that forms in the lee of Cairn Point during strong ebb flows was greatly suppressed with the expansion in place. The ebb flow character was altered significantly. This change will be discussed in much more detail later. In light of the altered eddy structure on spring ebb, at this location, the expansion doubled the time during which the current was in the ebb direction and reduced the time during which the current was in the flood direction (creating more balance between duration of flood and ebb). Ebb flows were generally stronger with the expansion in place, compared to existing conditions. It is interesting to note that the eddy is not nearly as strong during neap ebb conditions as it is during spring tides, presumably because the ebb currents that flow past Cairn Point that spawn the eddy are much reduced in strength for neap tide (lower tide range) conditions.

At Expansion Berth 6 station, Figures 47 and 59 show that the current speed did not change much at all during the neap-spring cycle, except at the end of ebb tide where, again, the eddy structure was suppressed during spring tide conditions. Flood flows throughout the entire spring-neap cycle were essentially unaltered. The expansion reduces the early peak ebb flows by a few cm/sec, at this location, a relatively minor change. As a consequence of the suppressed eddy in the latter stages of ebb flow, the expansion increased the time during which the current was in the ebb direction and slightly decreased the time during which the current was in the flood direction. The expansion constrains the flow to move along the dock face, thus the observed changes in direction throughout the tidal cycle.

At Expansion Berth 5 station, Figures 48 and 60 show that the current speed slightly increased on flood flows, with the expansion, by only a few cm/sec. Peak ebb currents early in the ebb cycle showed no change with the expansion in place. Again the eddy was suppressed during the later stages of ebb flow, and ebb currents were slightly higher with the expansion.

At Expansion Berth 4 station, Figures 49 and 61 show that the current speed increased with expansion, on both flood and ebb. Increases during flood were between 5 and 10 cm/sec. The eddy was suppressed, and current speed was increased and at the end of ebbing tide. The expansion eliminated the divergence in current direction during ebb tide that was associated with the eddy.

At Expansion Berth 3 station, Figures 50 and 62 show that the current speed was generally unaltered, and the current direction was generally unaltered, expect at the end of ebb tide when currents were slightly stronger with the expansion in place (a few cm/sec).

At Expansion Berth 2 station, Figures 51 and 63 show that the current speed during flood flow decreased by about 5 to 10 cm/sec during most of the spring-neap cycle (10 cm/sec during spring conditions, which is about a 10% decrease). Peak ebb flows were about the same, except at the end of ebb flow when suppression of the eddy resulted in slightly higher ebb flows with the expansion in place.

At Expansion Berth 1 station, Figures 52 and 64 show that the current speed increased slightly with expansion at the end of ebb tide, by a few cm/sec. During flood currents, the expansion decreased currents significantly (by about 15-20 cm/sec, or about 30% of the peak currents of 60 cm/sec). The strongest ebb flows that occur early in the cycle were unaffected by the expansion. In general, at the south side of the expanded dock, flood currents are decreased most significantly, whereas, flood currents are increased slightly along most of the northerly portions of the expanded dock.

At the Groin station, Figure 53 shows that on the flood tide, currents at the groin were reduced significantly with the expansion in place, as was the case for the Berth 1 station. The expansion tends to force flood flow out toward the center of the inlet, away from the dock face, decreasing flows at the southern end of the proposed dock. The momentum of the flood tidal flow in the inlet gorge appears to outweigh this effect further north along the proposed dock face, and currents are slightly increased on flood flow. Again, at the end of the ebb tide current speeds were slightly increased with the expansion in place, due primarily to suppression of the eddy.

At the Creek station, Figures 54 and 65 show that the expansion had little effect on currents, changing current speeds by a only few cm/sec at most, and not altering the directional pattern. Alterations to the current field are most significant right at the port, and changes are significantly reduced just a short distance to the south of the Port.

At Woronzof Flat 1, 2, and 3 stations, further south of the Port, Figures 55 through 57 show that the current speed was not altered. Also, current direction in general was not changed, except rarely in isolated instances for very brief periods of time. In general, changes in velocity at the three tidal flat locations can be considered to be negligible with the expansion in place.

The circulation pattern for a typical spring tidal cycle, for existing conditions, is described in some detail below to aid in understanding flow near the Port, and is best interpreted by viewing the flow field animations that accompany this report and are discussed later. Note differences between the north and south ends of the port vicinity, particularly along the dock face, and how they might influence sedimentation patterns within the harbor basin.

In general during flood flow, water moves from south to north rather uniformly along the Port, from north to south, as might be expected. Starting at low slack water (low tide), flow is slow and directed toward the north along the dock face. As the flooding tide progresses, the north-directed currents along the dock

face grow in strength and then wane in strength as high water slack tide is reached. This pattern is typical and intuitively expected. One might expect that during ebb flow, the water flows primarily to the south along the dock face, in response to the ebbing tide. That is the case in certain areas of the inlet, particularly the inlet gorge. However, that is not the case along some of the tidelands, including those near the Port. Initially, early in the ebb portion of the cycle, flow is to the south along the dock face as one might expect. But as the ebb flow past Cairn Point strengthens, the strong ebb current forms a large eddy, or gyre, south of Cairn Point, in which water circulates in a counterclockwise motion. The shape, extent, and strength of the eddy change during the ebb portion of the tidal cycle. The evolving counterclockwise flowing eddy causes the initially south-directed ebb flow to stop, and then reverse direction. So at peak ebb flow, water moves to the north along the dock face, not to the south as one might expect during an ebbing tide. This eddy grows in size with time on the ebb cycle, and by the time low tide slack water occurs, the eddy extends slightly past the south end of the Port. The weakly northerly-flowing water at the dock face due to the eddy gives way to increasingly stronger flood flow on the next incoming tide. It is interesting to note that the center of the gyre (expected to be a relatively stagnant water mass) initially advances south toward the port, reaches a position that is just south of the northern edge of the port, then reverses direction and heads back to the north and out toward the center of the inlet.

Figures 66 and 67 show the circulation pattern in the port vicinity at the beginning of ebb tide for the existing and with-expansion conditions respectively (again, spring tide conditions). It can be seen quite clearly from the Figures that for the existing condition, the counterclockwise eddy exists during spring ebb conditions to the north of the dock and to the south of Cairn Point. The eddy was not observed for the with expansion condition, for the same time period.

Figures 68 and 69 show the circulation pattern in the port vicinity, three hours after the ebb started, for the existing and with expansion conditions respectively. It can be seen that the eddy grew in size and extended to the south of the dock for the existing condition as seen in Figure 68. For the with-expansion condition, the eddy started to form as seen in Figure 69. Formation of eddy formation was lagged in time for the with-expansion case.

Figures 70 and 71 show the circulation pattern in the port vicinity at the end of ebb tide. It can be seen that the eddy moved toward the center of the inlet for both conditions but it extended more to the south for the existing condition.

Figures 72 and 73 show the circulation pattern in the port vicinity during high water slack tide for the existing and with expansion conditions respectively. The circulation pattern shows that the flow was flooding at the two sides of the inlet and was ebbing in the inlet center for both conditions.

Figures 74 through 77 show current vectors for the existing and with-expansion conditions overlaid on the current speed contours of the with-expansion condition. This display helps to show the change in current direction caused by the expansion. Figure 74 shows the current vectors during flood tide. It can be seen that the expansion caused the current, in front of the dock face, to be diverted away from the dock face at the southern end and toward the dock face at the northern end of the dock. Also the expansion changed the current direction in low-velocity areas such as on the tidelands and in areas with eddies. Figure 75 shows the current vectors during high water slack tide; and it can be seen that the expansion altered the current direction in low-velocity areas. Figure 76 shows the velocity fields during the beginning of ebb tide. The expansion diverted the flow slightly away from the dock face at the northern end of the dock face and toward the dock face at the southern end of the dock. Figure 77 shows the velocity fields during the end of ebb tide. The figure shows the change in current direction associated with the eddy south of Cairn Point.

Figures 78 through 80 show the current speed difference between the existing and with expansion conditions in the port vicinity area during flood, high water slack and ebb tides respectively. Note the scale shows changes in current speed of between + and – 20 cm/sec. Only in a few areas did the magnitude of the changes exceed +/- 20 cm/sec, and changes were generally restricted to the immediate vicinity of the expansion and at Cairn Point. Also note that white areas in these figures indicate regions where the changes in current speed are negligible, less than 4 cm/sec. Figure 78 shows that the expansion reduced the current speed at the southern end of the dock face and increased the current speed in front of the dock face during flood tide. Also the current speed at Cairn Point was increased with the expansion during flood tide. Figure 79 shows that the expansion caused the current speed at Cairn Point to increase in some areas and decrease in another area during high water slack tide. Figure 80 shows that the expansion increased the current speed in front of the dock face during ebb tide.

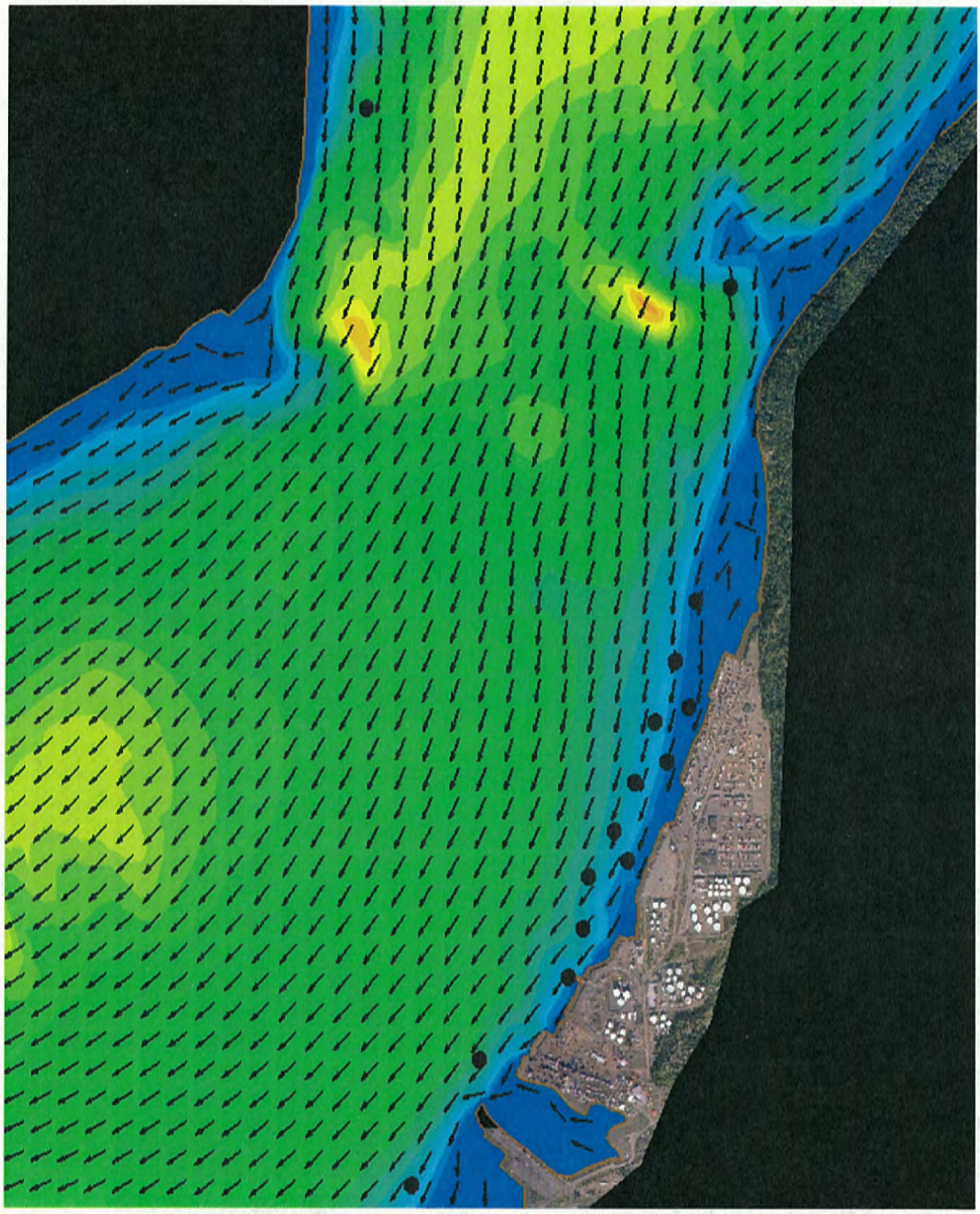

Figure 66 Existing Circulation Pattern at Beginning of Ebb Tide

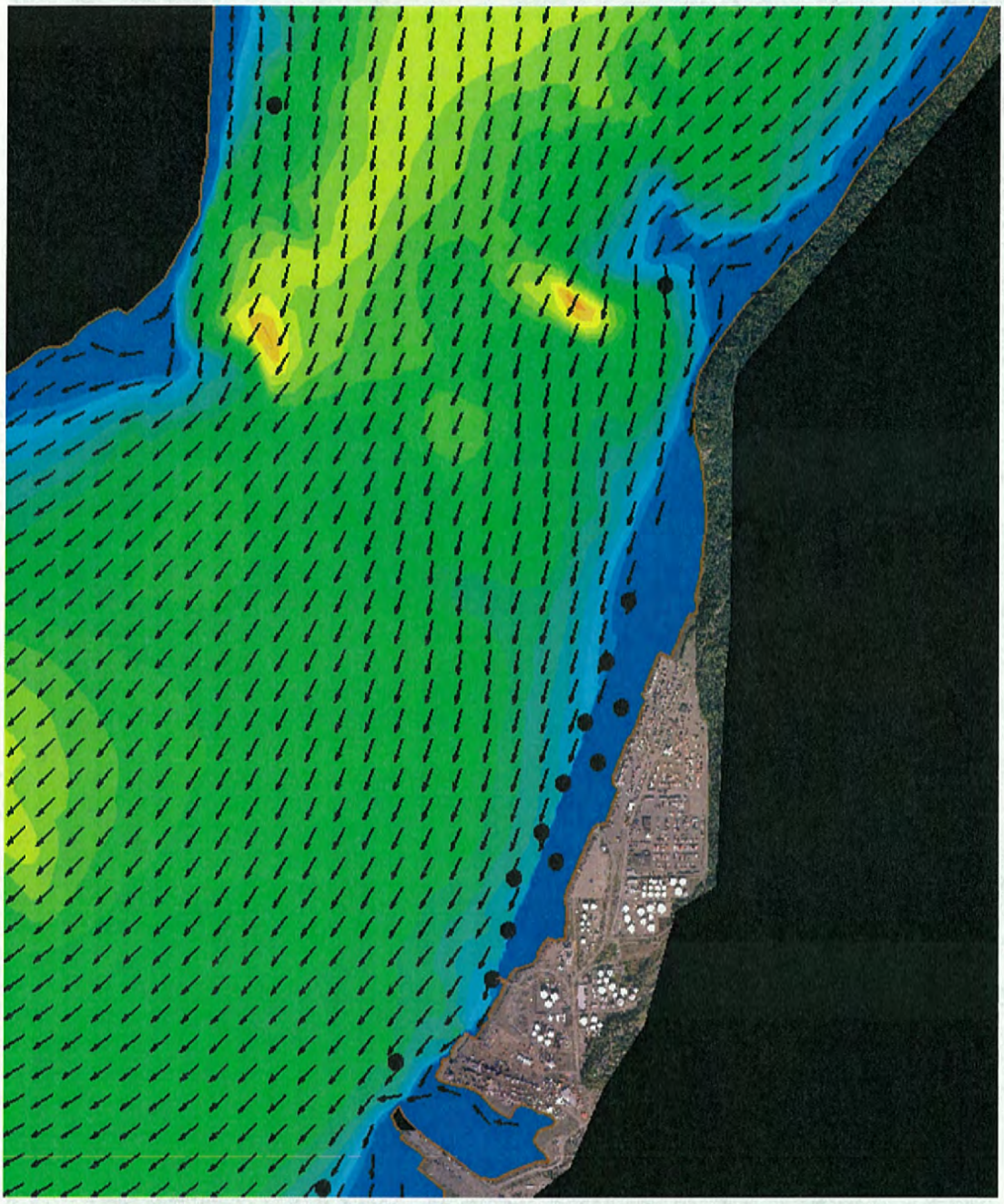

Figure 67 Circulation Pattern with Expansion at Beginning of Ebb Tide

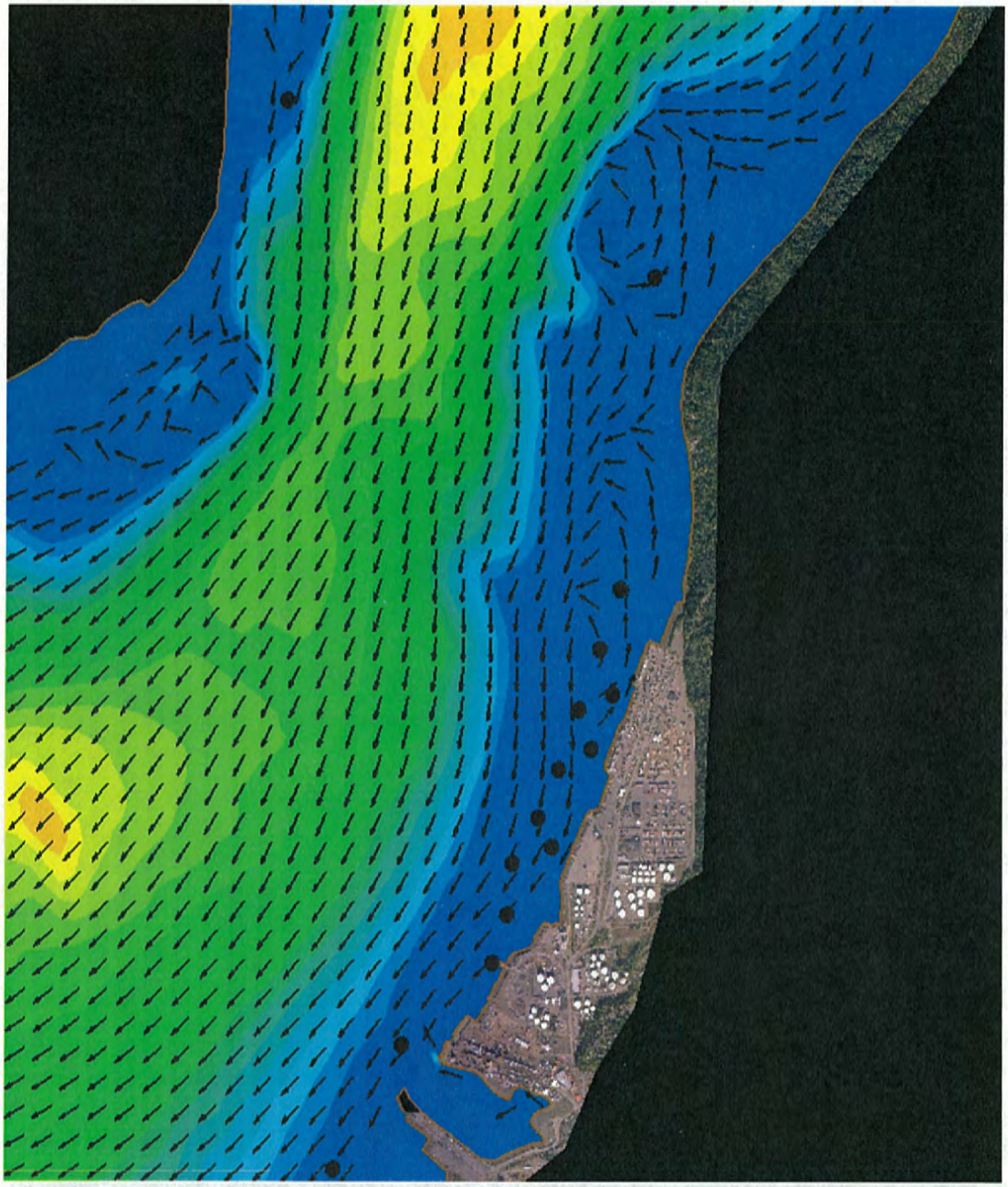

Figure 68 Existing Circulation Pattern During Ebb Tide

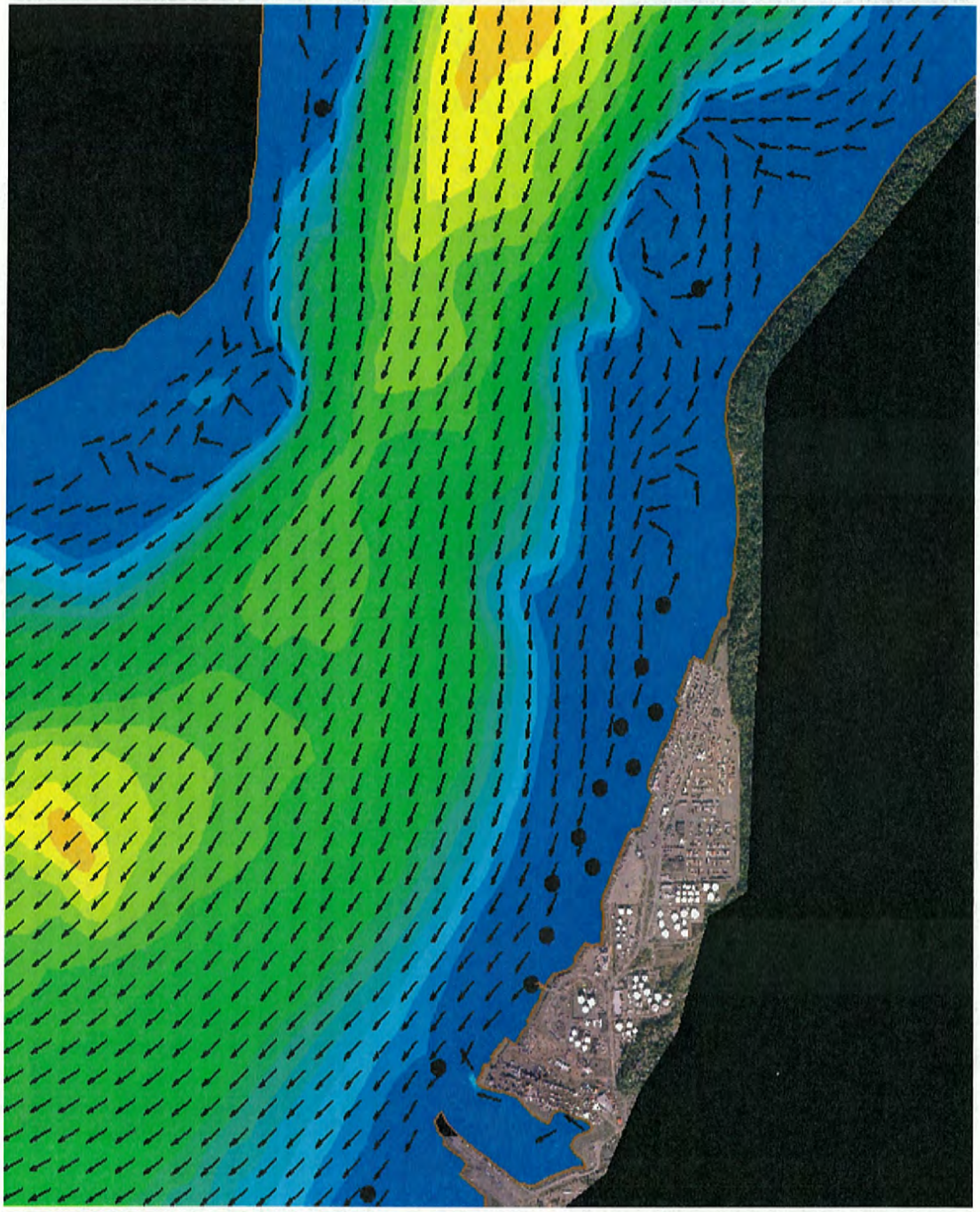

Figure 69 Circulation Pattern with Expansion During Ebb Tide

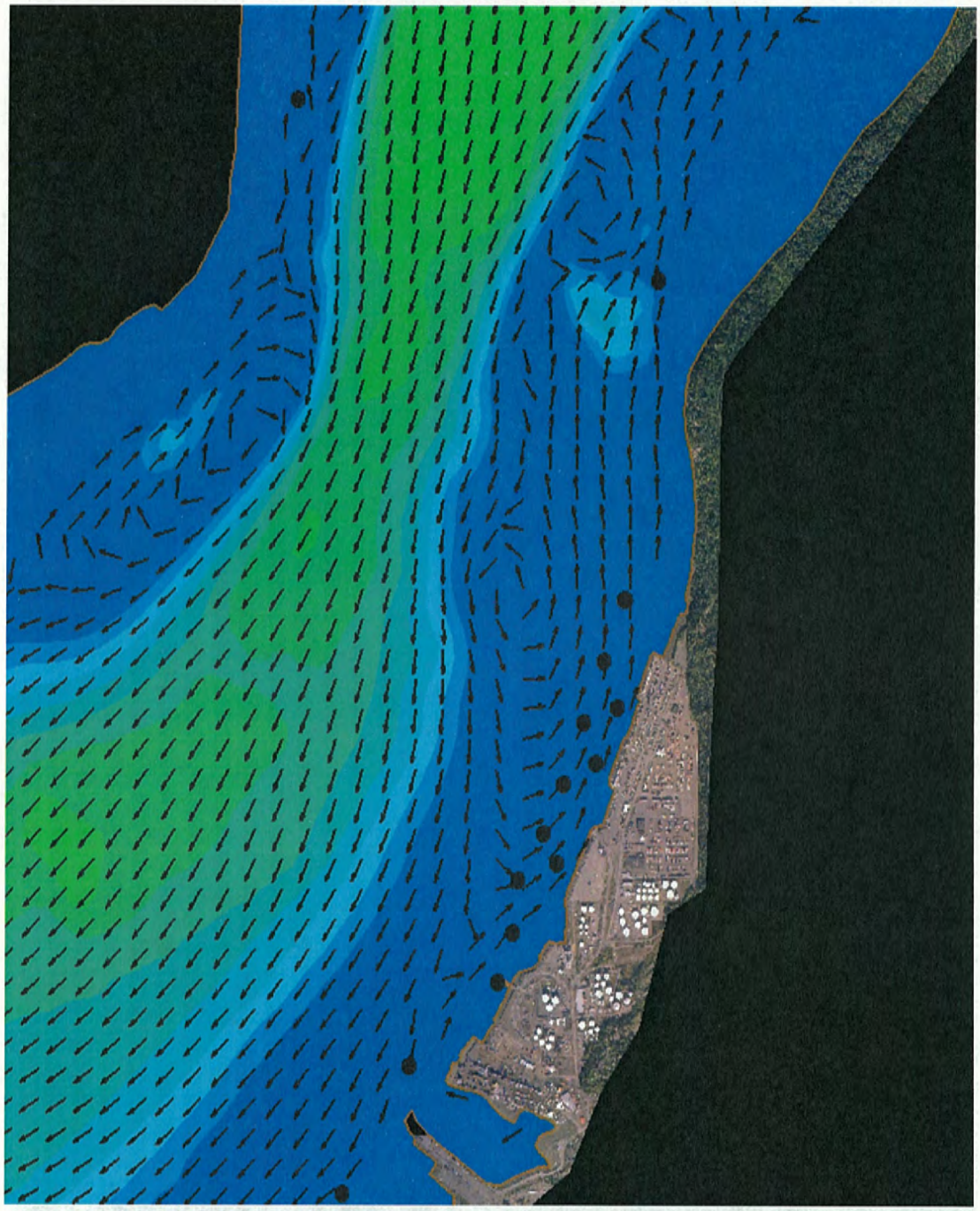

Figure 70 Existing Circulation Pattern During End of Ebb Tide

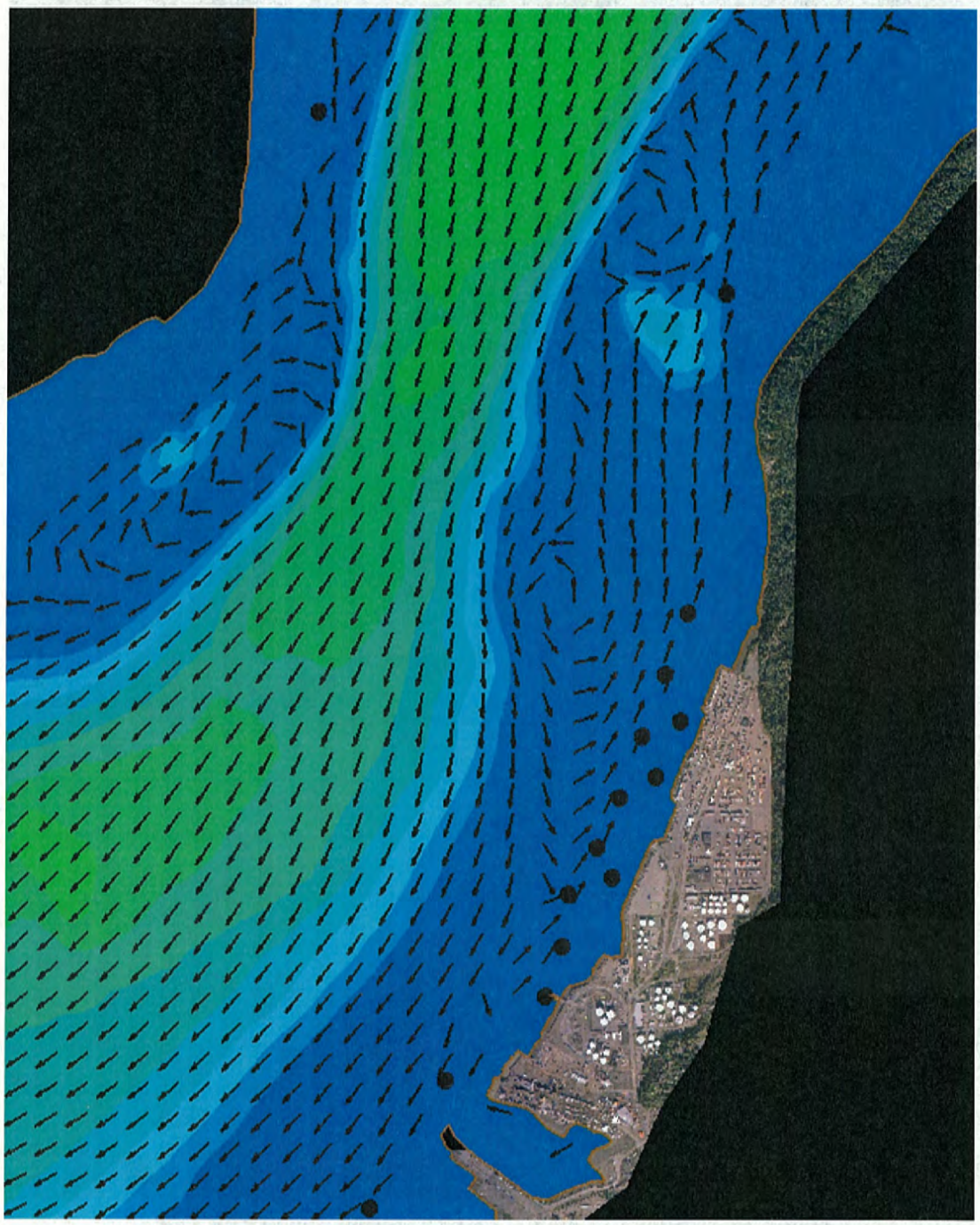

Figure 71 Circulation Pattern with Expansion During End of Ebb Tide

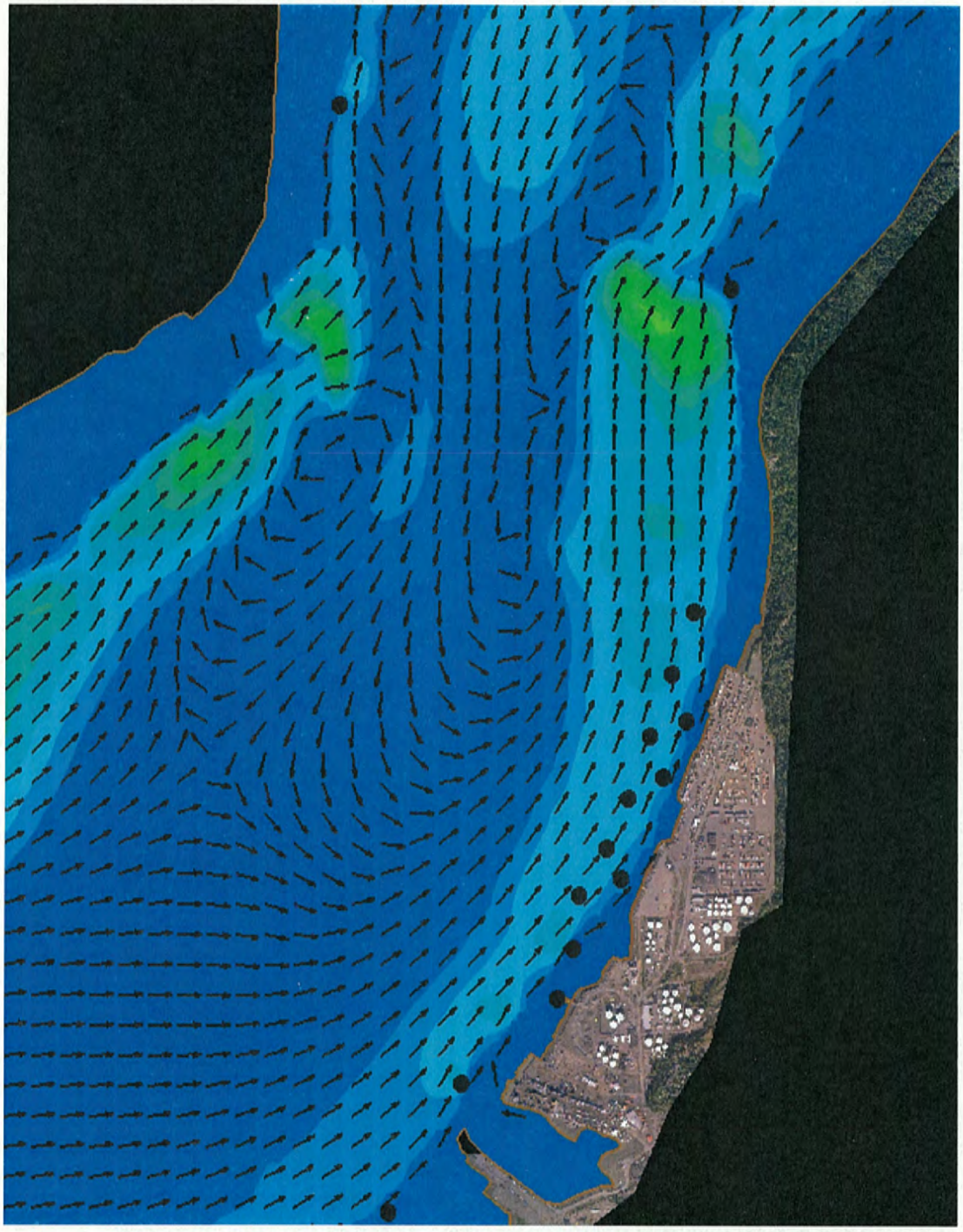

Figure 72 Existing Circulation Pattern During Low Water Slack Tide

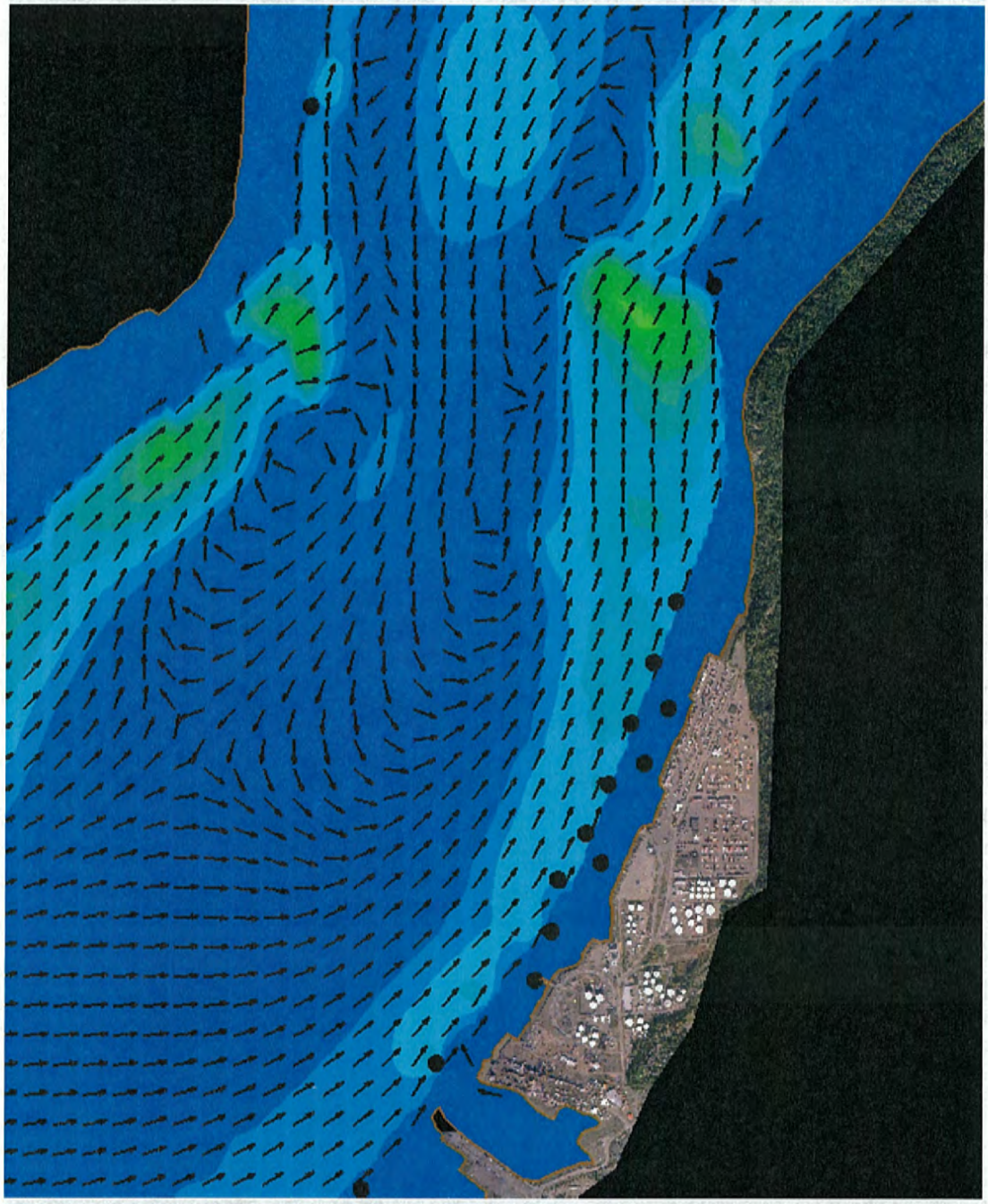

Figure 73 Circulation Pattern with Expansion During Low Water Slack Tide

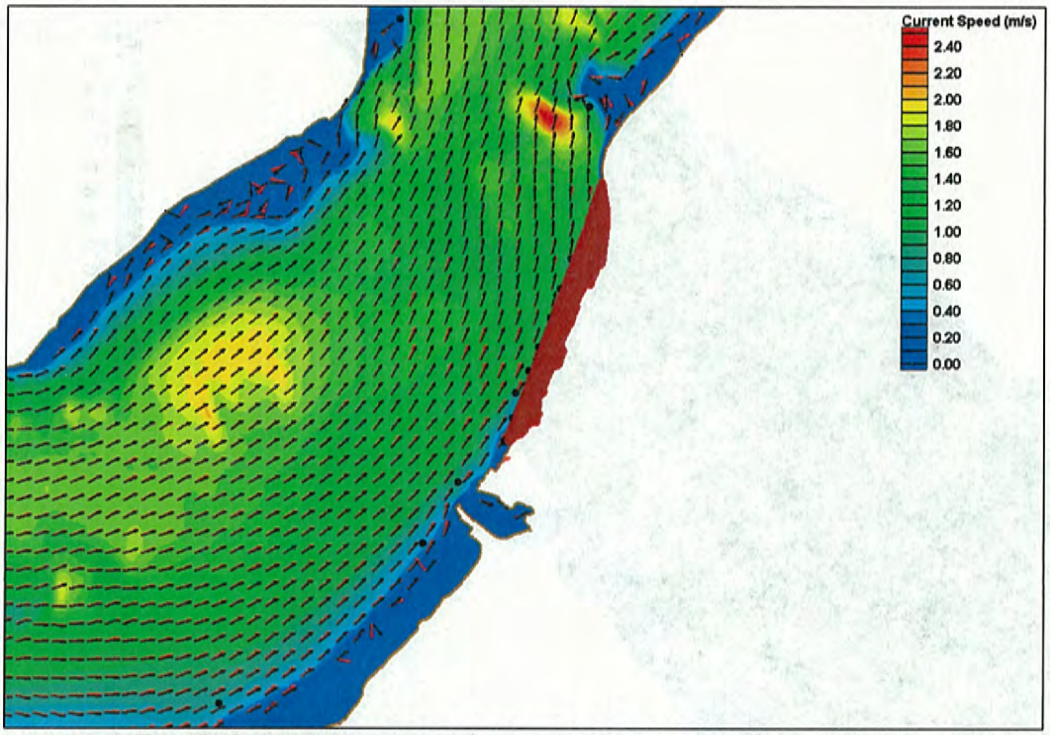

Figure 74 Existing (black) and with Expansion (red) Circulation Pattern During Flood Tide

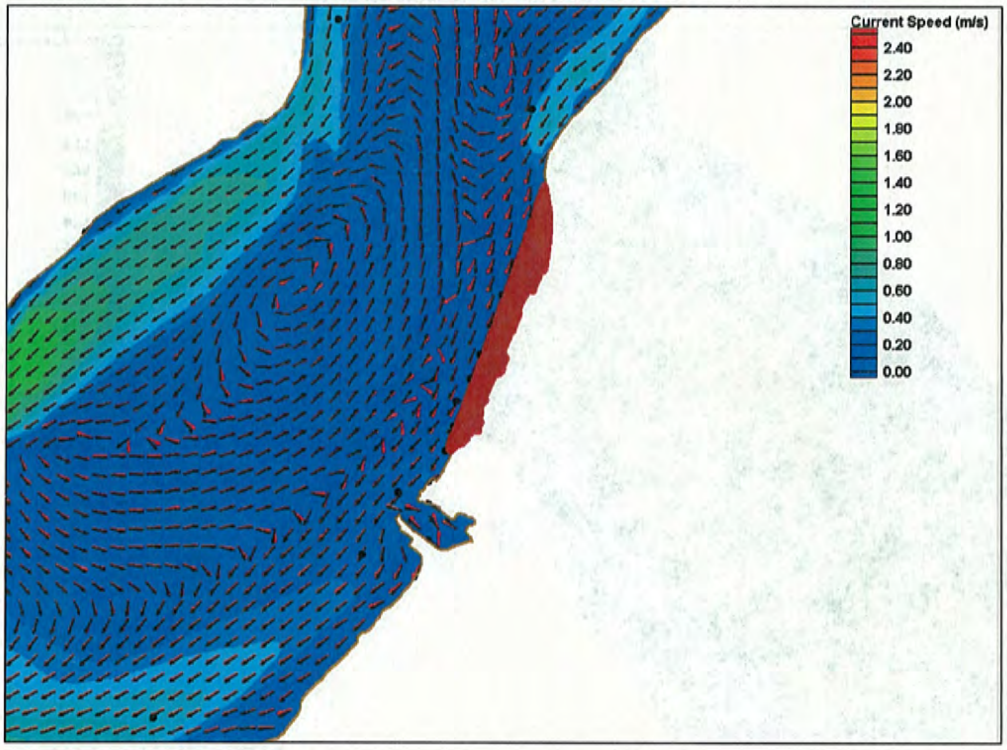

Figure 75 Existing (black) and with Expansion (red) Circulation Pattern During High Water Slack Tide

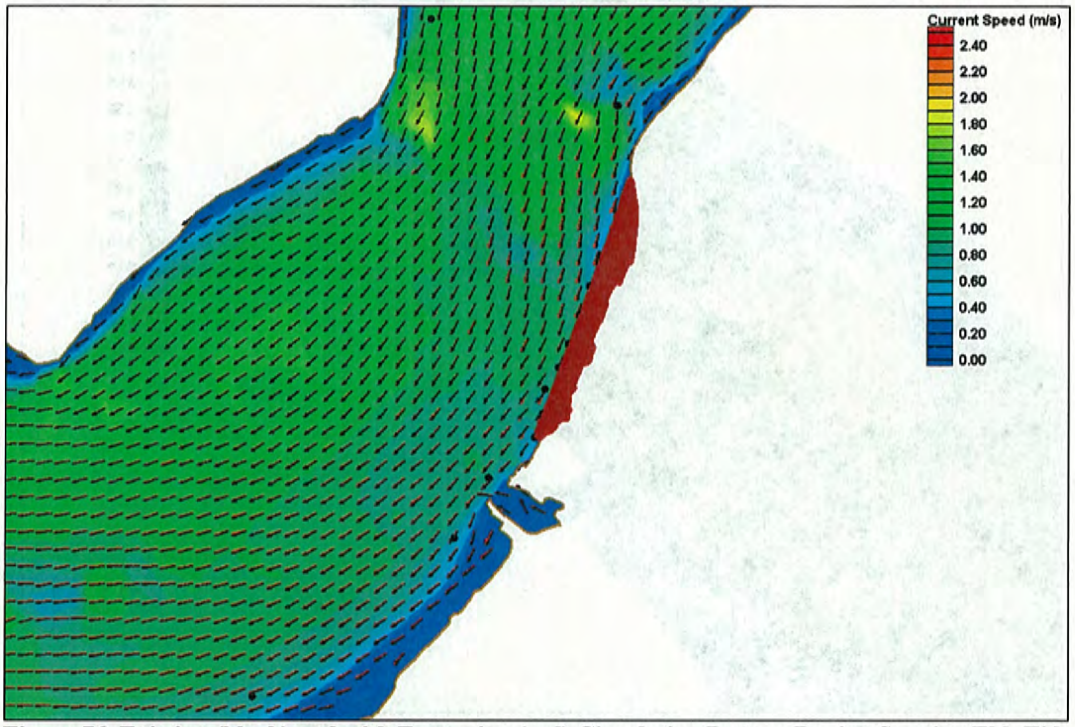

Figure 76 Existing (black) and with Expansion (red) Circulation Pattern During Starting Ebb Tide

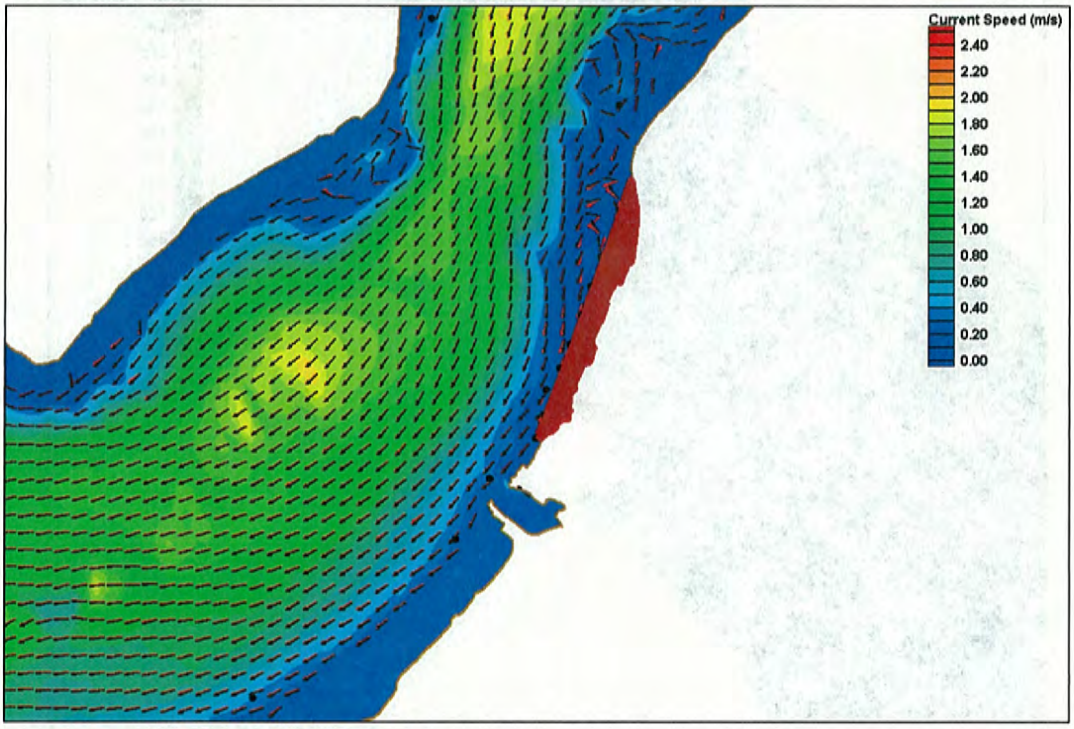

Figure 77 Existing (black) and with Expansion (red) Circulation Pattern During End of Ebb Tide

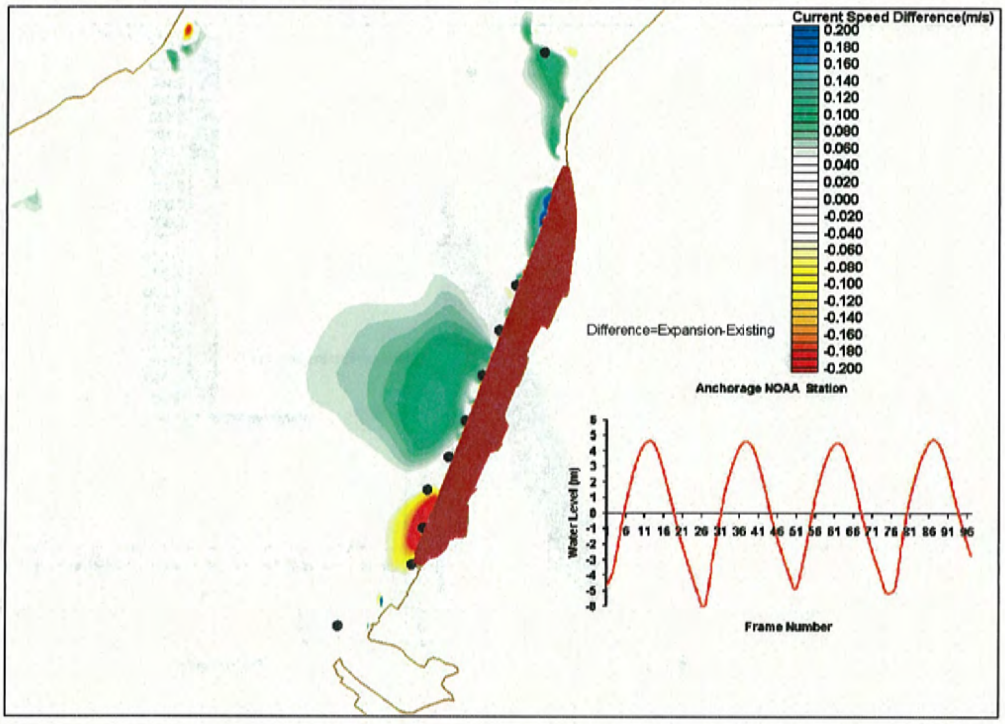

Figure 78 Current Speed Difference Plot During Beginning of Flood Tide

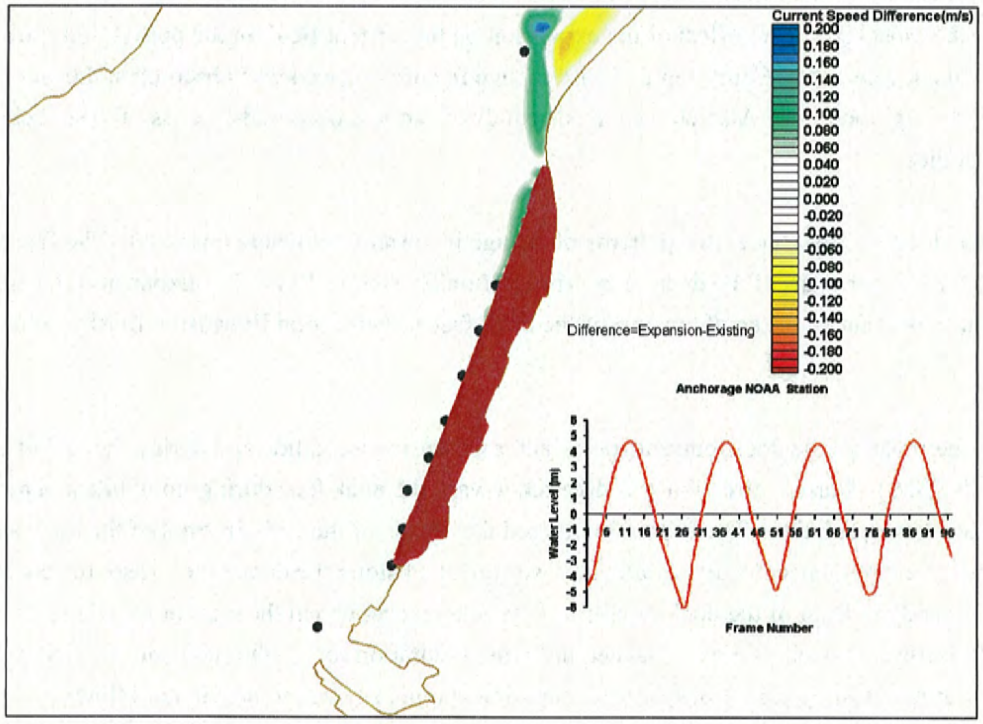

Figure 79 Current Speed Difference Plot During High Water Slack Tide

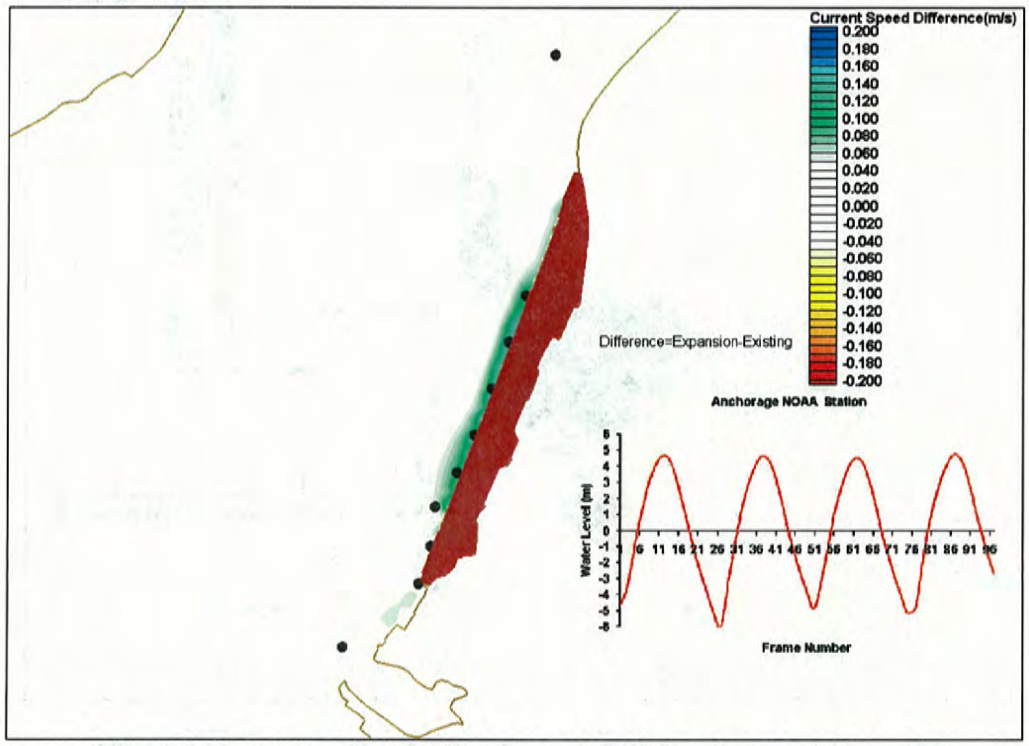

Figure 80 Current Speed Difference Plot During Ebb Tide

In general, the most significant effect of the expansion on the current field, in the port vicinity, was in front of the dock face and at Cairn Point. Some change in current speed was observed at the western side of the inlet during flood tide. Also change in current direction was observed in areas of weak velocity fields and eddies.

For the area along the dock face, two patterns of change in current field were observed. The first pattern dominated the northern part of the dock face (from station Expansion Berth 7 to Expansion Berth 4). The second pattern dominated the southern part of the dock face (from station Expansion Berth 3 to the Groin station).

For the northern part of the dock, current speed increased during flood tide and during the end of ebb tide (weaker ebb flows). Current direction was diverted toward the dock face during flood tide and away from the dock face during ebb tide. The expansion altered the details of the eddy in front of the dock and consequently the divergence in current direction was changed along the dock face. Also, the change in details of the eddy in front of the dock minimized the time during which the current was directed toward the north (the current becomes more balanced in terms of duration for northbound and southbound currents). For the existing conditions, current direction is more skewed to northbound flows.

For the southern part of the dock, current speed decreased during flood tide and during the start of ebb tide and increased during the end of ebb tide. Current direction was diverted away from the dock face during flood tide and toward the dock face during ebb tide.

Sediment Transport Implications of the Proposed Full Expansion – At the Port

The harbor basin at the Port of Anchorage is basically a dredged notch in the tidal flat. Sediment loads in upper Cook Inlet are quite high; spring thaws occur and accompanying river discharges introduce considerable amounts of sediment to the system. Erosion in other areas of upper Cook Inlet probably also contribute significant sediment loads to the system which subsequently are transported through the system as well (a redistribution of existing sediment deposits, such as erosion of Cairn Point shoals or the changing channel/shoal system south of and across the inlet from Point Woronzof). As such, natural sedimentation processes act to fill the notch each spring and summer season, probably working to recreate the general tidal flat structure in this region which is in some state of quasi-equilibrium, or balance, with the predominant tidal currents.

The shoal features that form at the landwardmost corners of the north and south ends of the harbor basin have distinctly different growth characteristics. That fact suggests that hydrodynamics at the two locations are also different, because hydrodynamic forces drive the sedimentation patterns. At the south end, the shoal begins to form as a more elongated, shore-parallel feature; and its extent grows primarily in the alongshore direction, starting at the south wing cut and gradually growing in a northerly direction. The shoal's major axis is primarily oriented in the alongshore direction, at least initially. The shoal begins to form in May, and by July the crest elevation of the feature reaches 5 to 6 feet above the authorized depth (the current authorized depth of 35 ft below MLLW). The shape of the north shoal is different; it is fan-shaped, not elongated. It begins in May as a deposit in the corner where the dock face meets the wing cut and expands radially outward along and away from the dock face. This deposit does not have a well-defined major axis of orientation as is the case for the south shoal. In terms of area extent, the north shoal is larger than the south shoal; and by July, its crest elevation can reach 10 ft above authorized depth. As each of the two shoals grows in size during the summer, a ridge, or sill, begins to form between them. The ridge slowly grows and forms a bridge between the two shoals. As the ridge forms and grows, sedimentation between the sill and the dock face increases.

Sediment dynamics at, and in the vicinity of, the Port of Anchorage are complex and not well understood. Most likely sedimentation in the harbor is due to several factors, including alongshore movement of sand, silt, and fluid muds that are formed on the shallow tidelands, as well as sediments that settle to the bottom during relatively quiescent times in the tidal cycle (suspended sediment loads in the system are considerable). Without additional studies devoted to the issue of sediment dynamics, which have been proposed, it is unlikely that they can be understood with a high degree of confidence. However, to support the environmental assessment, the influence of the proposed port expansion on flow and

circulation was made; and based on those results, a cursory assessment of the impact of the port expansion on sedimentation harbor was also made.

The tidal current characteristics at the north and south ends of the dock face are different. At the south end of the dock face, where the south shoal develops, the flow is generally back and forth in an alongshore direction. The persistent back and forth alongshore movement of water is consistent with formation of a shoal feature that has a major axis in the alongshore direction (more of a linear feature). Flows are stronger on flood (to the north) than on ebb. This pattern is consistent with formation of a shoal, where strong currents most likely sweep sediment on flood flow (either moving in as bed load or as a fluid mud) into the harbor region; and on ebb, forces for removing sediment are lessened. Gravity (due to the sloping bed from the shallow tide flats to the deeper dredged basin) also promotes sediment movement into the basin, and retards sediment movement back out of the basin. In this way, the topographic depression of the basin is likely to "trap" sediment transported into it from the adjacent flats. There seems to be less time during which currents are very low at the south side of the Port, relative to the north side of the Port. In general, except within eddies, the flow regime in upper Cook Inlet and near the Port is energetic most of the time. Suspended sediment load in the system is most likely to settle out during very low flow conditions, but settling also depends on the grain size of the sediments in suspension.

At the north side of the dock face, conditions are quite different, compared to the south side. On flood flow, conditions are consistent with sediment being transported to the north throughout the flood cycle. Sediments that enter the basin from the south and are able to be transported to the north probably tend to accumulate at the north side of the basin because they must overcome gravity to be able to leave the basin and enter the shallow adjacent tidelands. The angled wings in the basin notch may help divert the sediments further out into the basin on flood flow. In the early stages of the ebbing tide, flow is directed to the south at the north side of the harbor. At this time, and for a rather short duration, flow has its highest southerly magnitude (but weaker magnitude compared to flood currents). Sediment being transported around Cairn Point and along the tidal flat (transport along the bed or as fluid mud) is most likely to enter the basin under this current action. But rather soon into the ebb cycle, flow conditions at the north shoal become dominated by the presence of the gyre discussed above. The gyre is a relatively weak current environment, and the core of the gyre has the weakest currents. While the ebb gyre forms, grows in extent, and then begins to migrate offshore, flow is to the north a majority of the time at the north end of the Port. As the ebb cycle advances, the core (center of the formed gyre) moves southward just to the northern extremity of the basin, then reverses direction and moves northwest away from the dock face toward the middle of the inlet. This evolution of the eddy creates currents that are relatively weak, but they predominately act to transport sediment (probably those in suspension) that might be moving around Cairn Point into the harbor and to the north, in a counterclockwise, rotary type of action. The gyre generally has weak flows. Fine sediments are most likely to settle out in the low flows that characterize the gyre, particularly the core. If settling of suspended sediment is an important

sedimentation process at the Port, the slow moving gyre is expected to be a spreading mechanism for deposition of material and conducive to sedimentation in the northern portion of the harbor basin. This process would also be consistent with the observed growth of the north shoal as a larger, fan-shaped feature, having a less well-defined orientation or major axis. Due to the low flows associated with the gyre, and a moving gyre, this pattern may produce the wider shoal deposit that is observed on the north side of the Port, compared to the south side. The flow pattern at the north side of the Port is dramatically different from the flow pattern on the south side, which is consistent with the dramatic difference in shoaling pattern at the two locations. The dredged wing at the south end of the basin, may not be as effective as the northern wing because ebb currents at the south end of the basin are not nearly so strong as flood currents at the northern wing and they may not be strong enough to have the wing promote sediment movement back out into the basin and into a higher current regime.

Also of interest is the current shear line that forms just off the dock face at a certain time near slack high water of the tidal cycle. At the Port's location in upper Cook Inlet, when the middle of the inlet gorge is finishing the flood stage near slack high water, and flow in the gorge is still directed to the north in the flood direction, ebb flow is beginning on the tidal flat along the Port. At this point in the tidal cycle, a very abrupt velocity shear zone is formed just off the dock face. It is hypothesized that the shear line represents a low flow zone (stagnant zone) where sediment might tend to settle out. This shear line has been observed on aerial photography. The location of the velocity shear zone is very similar to the location where the sediment ridge forms within the harbor basin. There may be a connection between the two; but without further study, a cause and effect relationship between the shear line and the sedimentation ridge is uncertain.

The Port expansion was modeled as a solid fill, unlike the present pile-supported dock, so its inclusion in the hydrodynamic model reflects a loss of tidal flat area. If the harbor is constructed as a pile structure, results might be quite different than those presented here. For without-expansion conditions, there is water moving along the tidelands in the port vicinity. Because of the expansion, and its effect of reducing the area that is available for along-shore moving water to flow, one would expect the expansion to increase current speeds along the expanded dock face (free surface gradient associated with the tide wave forcing water movement through a smaller cross-sectional area). That was the hypothesis formed at the outset of this study. But it is also important to note that the vast majority of tidal flow moves through Knik Arm, past the Port, within the deep tidal gorge. The flux of water through the gorge dwarfs the flux that moves along the tidelands. Flow in the gorge, which the expansion does not affect much at all, has significant momentum which also dictates flow past the expanded dock face. The increase in current speeds due to the Port was not expected to be great, and results showed that it was not.

With the expansion in place, flood flows are increased along most of the proposed dock face, except at the south end, where current speeds on flood are decreased. This suggests that the potential for currents to transport sediment along the bed to the north and into the harbor basin is also decreased. On flood, the

expansion produces a pattern of increasing flood current strength from south to north along the dock face. This pattern, i.e., reduced flood currents to the north at the south end, and increased flood currents to the north at the north end, generally suggests a divergent flow environment which is expected to produce a reduction in sedimentation potential along much of the dock during flood flows. However, gravity effects induced by dredging a deeper basin out of shallow tidelands will still act to retain sediments transported into the basin, within the basin. The higher flows that will be experienced at the expanded dock face may help the effectiveness of dredged wings to move sediment back out into the basin and into even stronger flows. Along much of the dock face, flood currents are increased for the proposed expansion. Higher flows also suggest decreased likelihood that sediments can settle out of suspension.

A seemingly more significant change occurred during ebb conditions. The presence of the expansion greatly alters the formation of the gyre during the ebb portion of the tidal cycle. The flats are removed with the expansion in place. The expansion causes formation of the gyre to be suppressed, and its formation occurs much later in the ebb tidal cycle. Flows are directed to the south on ebb for a larger percentage of time at higher strength, along much more of the dock face, compared to the without-expansion conditions when weaker flows were directed toward the dock and into the northern corner of the basin. This reduces the time during which flows are weak, reduces the time during which a gyre is present at the north end of the harbor basin, and reduces the time when a weak gyre core is present at the north side of the harbor. From a suspended sediment perspective, this suggests that there will be a hydrodynamic regime in front of the dock face that is less conducive to settling of suspended sediments. So, if settling is a contributor to sedimentation within the basin, which is expected, then sedimentation due to this particular process is expected to be reduced with the expansion in place. The increase in strength and duration of south-directed flows may promote more near-bed sediment transport toward the basin, compared to existing conditions; but note that these ebb currents are weaker than the flood currents at the south end of the basin. And during the increased time that ebb currents are directed to the south, the magnitude of current increases from north to south indicating a divergent velocity zone that is probably conducive to reducing sedimentation along much of the dock face. Overall, the proposed expansion appears to have less potential for sedimentation that the existing port, which is probably not surprising in light of the fact that the filled expansion moves the dock face out into deeper water and into a higher flow regime.

Animated Graphics

Animated flow circulation patterns were prepared with snapshots of flow fields every half-hour for the study area during two days of spring tide (August 10.5-12.5, 2002).

Animations were prepared for four areas. Area 1 shows the region between Point Woronzof and Cairn Point (Figure 81). Area 2 shows the refined area where ADCIRC grid resolution was increased (Figure

82). Area 3 shows the dock area as seen in Figure 83 and area 4 shows the area between the creek and the groin (Figure 84). Depth contours are also shown in these figures.

Two types of animations were prepared for each area. The first animation shows frames of water level contours and scaled current vectors and the second shows current speed contours and fixed vectors of current direction. The current speed contours with fixed vector lengths show current patterns and structure well, but the reader must remember that the vectors are not scaled to velocity magnitude as they are in the first type of animation. Current speed difference animations were prepared for Areas 1 and 3.

Also three drogue animations were prepared to show the path line of a water particle released in front of the port (at the dredging site), at the south end of the dredge disposal site, and in the center of dredged disposal site. The drogue plots suggest that sediment released at the disposal site, and which is retained in suspension for the entire time, does not appear to be transported in a net sense south toward the tidal wetlands south of the port (note, the drogues do not have a settling speed as sediment particles would). The drogue plots of releases within the disposal area suggest the particles move toward the Port, not south toward the flats, and then to the north. And the drogue plot showing a particle released at the Port quickly moves toward the north further up into Knik Arm away from the Point Woronzof tidelands and away from the wetlands that are located behind the flats. Table 1 shows a list of all the prepared animations.

Table 1 Animated Flow

Name	*Grid Condition*	*Area*	*Graphics*
wor-wl-cur	Existing	1	water level + current
wor-cur	Existing	1	current vector
wor-wl-cur-exp	Expansion	1	water level + current
wor-cur-exp	Expansion	1	current vector
all-dif-.5	Expan - Existing	1	current difference
ref-wl-cur	Existing	2	water level + current
ref-cur	Existing	2	current vector
ref-wl-cur-exp	Expansion	2	water level + current
ref-cur-exp	Expansion	2	current vector
ref-dif-pt	Expan - Existing	2	current difference
dock-wl-cur	Existing	3	water level + current
dock-cur	Existing	3	current vector
dock-wl-cur-exp	Expansion	3	water level + current
dock-cur-exp	Expansion	3	current vector
creek-wl-cur	Existing	4	water level + current
creek-cur	Existing	4	current vector
creek-wl-cur-exp	Expansion	4	water level + current
creek-cur-exp	Expansion	4	current vector
port-drogue-exp	Expansion		drogue flow
dis-cnt	Expansion		drogue flow
disp-s	Expansion		drogue flow

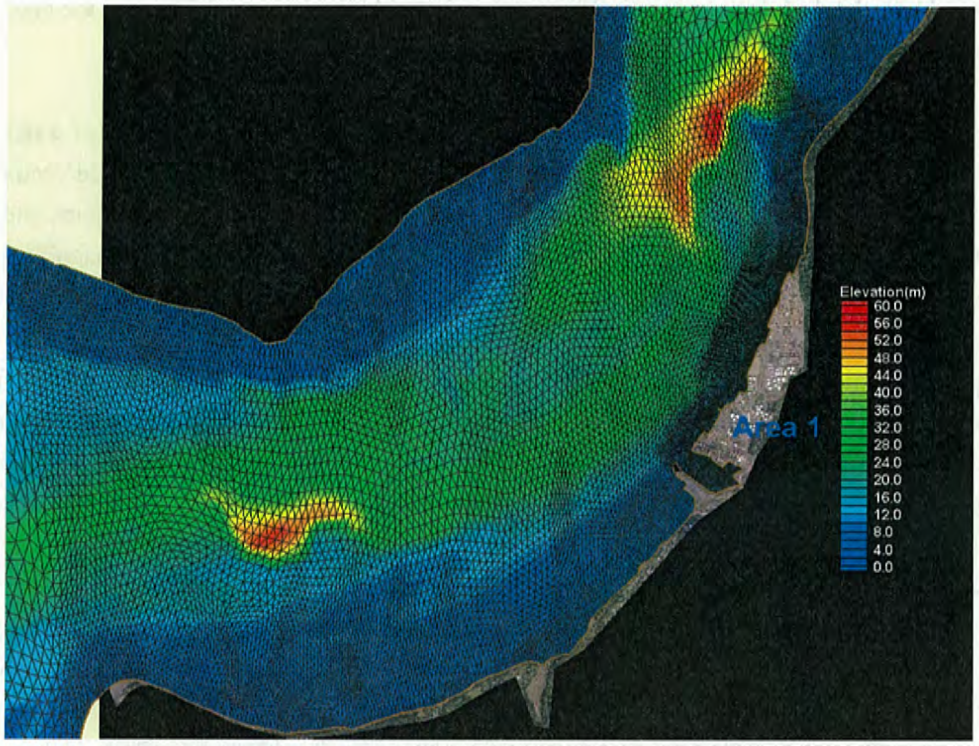

Figure 81 Area 1

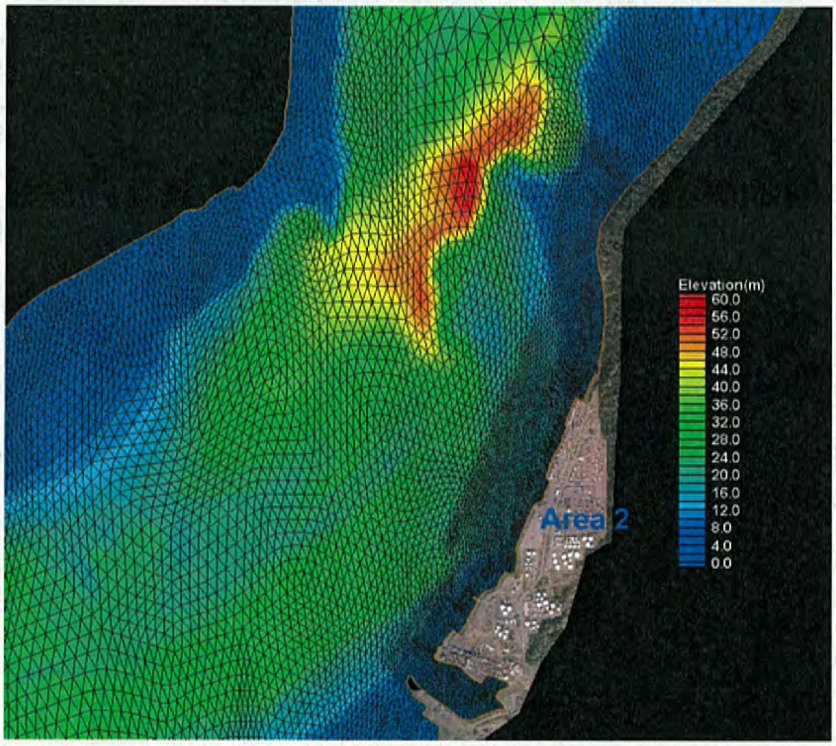

Figure 82 Area 2

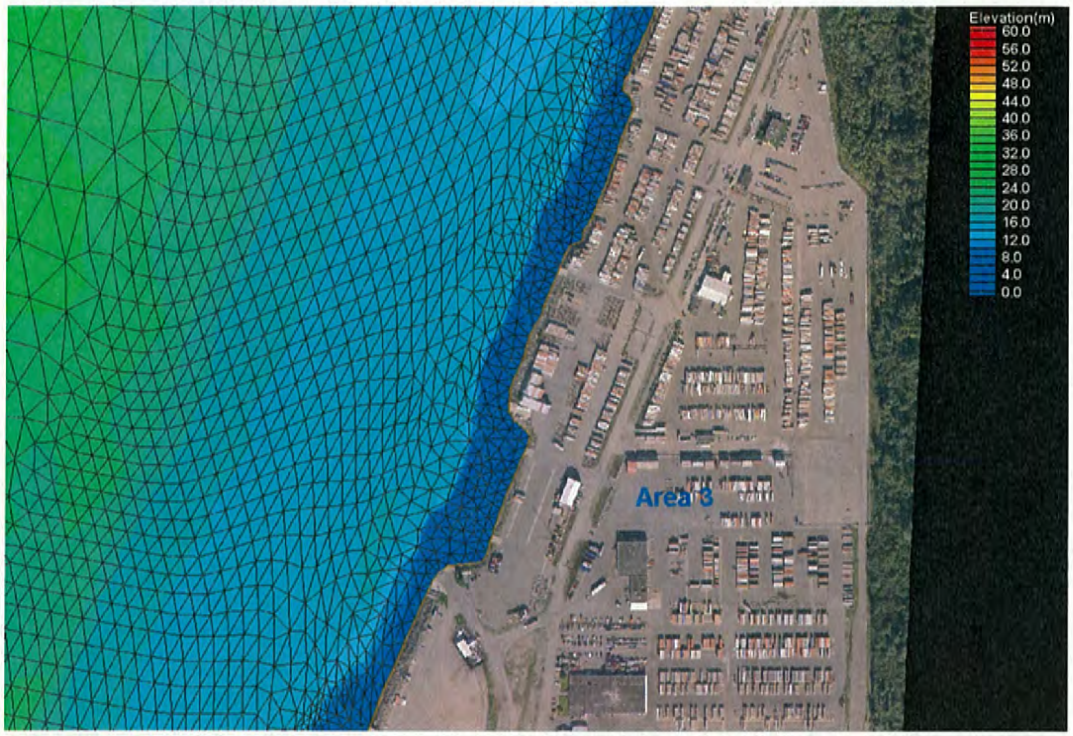

Figure 83 Area 3

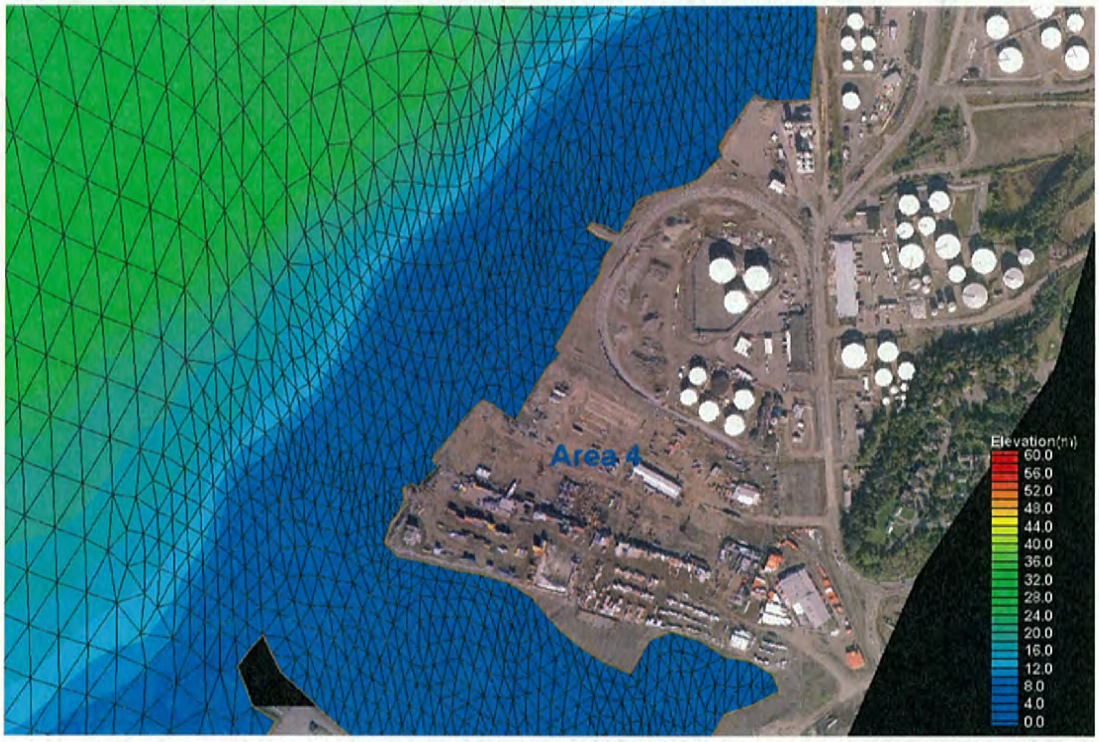

Figure 84 Area 4